ELSEVIER

Coordination Chemistry Reviews
214 (2001) 43–90

COORDINATION CHEMISTRY REVIEWS

www.elsevier.com/locate/ccr

Structural overview of technetium compounds (1993–1999)

Giuliano Bandoli [a,*], Alessandro Dolmella [a], Marina Porchia [b], Fiorenzo Refosco [b], Francesco Tisato [b]

[a] *Dipartimento di Scienze Farmaceutiche, Via Marzolo 5, I-35131 Padova, Italy*
[b] *ICTIMA, Consiglio Nazionale delle Ricerche, Corso Stati Uniti 4, I-35127 Padova, Italy*

Received 18 April 2000; received in revised form 14 July 2000; accepted 13 September 2000

Contents

* Corresponding author. Fax: + 39-049-827 5345 (5366).
E-mail address: bandoli@dsfarm.unipd.it (G. Bandoli).

PII: S0010-8545(00)00384-2

Abstract

This paper investigates the structural aspects of technetium-containing complexes. The focus is on the description of the various coordination environments around the technetium center. The complexes are divided according to the coordination sphere and the most significant structural parameters are reviewed and discussed. The review covers the crystallographic determinations published in the years between 1993 and 1999.

Keywords: Low-valent Tc; Metal–nitrogen multiple bonds; Oxo-complexes; Technetium complexes; X-ray structures

Nomenclature

14S4	1,4,8,11-tetrathiacyclotetradecane
16S4	1,5,9,13-tetrathiacyclohexadecane
18-ane-S_6	1,4,7,10,13,16-hexathiacyclooctadecane
18S6	1,4,7,10,13,16-hexathiacyclooctadecane
20-ane-S_6-OH	3,6,9,13,16,19-hexathiacycloicosanol
9-ane-S_3	1,4,7-trithiacyclononane
BATO	boronic acid adducts of technetium dioximes
BAT-PPP	bis(aminothio)-phenylpiperidinate (3 −)
BBB	blood brain barrier
biguan	1,1-dimethylbiguanide (1 −)
CN-*t*-bu	*tert*-butylisonitrile
Cp	cyclopentadienide (1 −)
Cp*	pentamethylcyclopentadienide (1 −)
CTA	cyclic tetraalaninate (4 −)
CYS–OEt	L-cysteine ethyl ester (1 −)
depe	1,2-bis(diethylphosphino)ethane
DIARS	*o*-phenylenebis(dimethylarsine)
dmdc	dimethyldithiocarbamate (1 −)
$(dmg)_3$BTol	tris(dimethylglioxime)tolylborate (2 −)
dmit	isotrithionedithiolate (2 −)
dmpe	1,2-bis(dimethylphosphino)ethane
DPhF	diphenylformamidinate (1 −)
dppe	1,2-bis(diphenylphosphino)ethane
dppm	bis(diphenylphosphino)methane
dtc	*S*-methyl-2-methyldithiocarbazate (1 −)
dtdc	5,8-dithiadodecane
DtolF	di-*p*-tolylformamidine (1 −)
e=dt	ethenedithiolate (2 −)
edt	ethanedithiolate (2 −)
Et_2dtc	diethyldithiocarbamate (1 −)

Et_2dtp	*O*,*O*′-diethyldithiophosphate (1 −)
Etxan	ethylxanthate (1 −)
hdto	8-hydroxy-3,6-dithiaoctan-1-olate (1 −)
HINYC	hydrazinonicotinamide
HN=NPh-*t*-bu	*p*-terbutyl phenyl diazenido
malt	maltolate (1 −)
MAAG	mercaptoacetylalanylglycylglycinate (4 −)
MAG_2	bis-mercaptoacetylglycinate (4 −)
MAG_3	tris-mercaptoacetylglycinate (4 −)
MAG_3OMe	tris-mercaptoethylglycine mono methyl ester (4 −)
Me_2bpy	4,4′-dimethyl bipyridine
Me_2dtp	*O*,*O*′-dimethyldithiophosphate (1 −)
mnt	1,2-dicyanoethene-1,2-dithiolate (2 −)
N=NPh	phenyldiazenido (2 −)
$N{=}NPh_2$	1,1-diphenylhydrazido
N=NPhCl	*p*-chlorophenyl diazenido (2 −)
N=NPy	2-hydrazinopyridine
N_2S_2DADS	1,2-bis(2-thiaacetamido)ethanate (3 −)
N^{isopr}Ar	2,6-diisopropylphenylimido
N^{Me}Ar	2,6-dimethylphenylimido
NPh	phenylimido (2 −)
PO	(2-diphenylphosphino)phenolate (1 −)
PN(etOMe)P	bis(diphenylphosphinoethyl)methoxyethylamine
PN(Pr)P	bis(diphenylphosphinoethyl)propylamine
PNH_2	(2-diphenylphosphino)benzeneamine
POOP	1,8-bis(diphenylphosphino)-3,6-dioxaoctane
POP	bis[(2-diphenylphosphino)ethyl]ether
PPh_2py	diphenyl(2-pyridyl)phosphine
$PyPPh_2$	pyridyl-diphenylphosphine
pyr	pyrrolidine
salen	*N*,*N*′-bis(salicylidene)ethane-1,2-diaminate (2 −)
Sbz	benzylthiolate (1 −)
SCP	$^{-}SCH_2P^{+}(CH_3)_2(CH_2)_2P(S)(CH_3)_2$
S_2CPh	dithiobenzoate (1 −)
S_3CPh	perthiobenzoate (1 −)
Smetetraz	2-mercapto-methyltetrazolate (1 −)
SN(etNEt_2)S	*N*-ethylaminodiethyl bis(2-mercaptoethyl)aminate (2 −)
SN(etpip)S	*N*-ethylpiperidine bis(2-mercaptoethyl)aminate (2 −)
SN(etSEt)S	*N*-ethylthioethyl bis(2-mercaptoethyl)aminate (2 −)
SNN(pyr)	*N*-(2-mercaptoethyl)(2-pyrrolidine)ethylaminate (2 −)
SPh	benzenethiolate (1 −)
SPhBr	*p*-bromo benzenethiolate (1 −)
SPhOMe	*p*-methoxy benzenethiolate (1 −)
$(SPPh_2)_2N$	bis(diphenylthiophosphoryl)amidate (1 −)
Spy	pyridine-2-thiolate (1 −)

SSS	3-thiapentane-1,5-dithiolate (2 −)
STol	*p*-methyl benzenethiolate (1 −)
thiuram	cyclopentamethylenedithiocarbamate (1 −)
thoz	2-(2′-hydroxyphenyl)-2-thiazolinate (1 −)
tn	trimethylenediamine
tosylate	*p*-toluenesulfonate (1 −)
tpy	2,2′,2″-terpyridine
Z-Ala-dtc	*Z*-Ala-*S*-methyl, 2-methyldithiocarbazate (2 −)
Z-Val-dtc	*Z*-Val-*S*-methyl, 2-methyldithiocarbazate (2 −)

1. Introduction

This review describes the structural chemistry of the coordination complexes of technetium. The goal is to provide an exhaustive literature coverage of the 7 year period 1993–1999. The survey is based on data recovered from Chemical Abstracts, but all major pertinent chemistry journals have been independently investigated. In addition, the most recent version (5.18, October 1999) of the Cambridge Crystallographic Database (CCDC) [1] has been searched extensively. Finally, recently published X-ray structures that have not yet been deposited into the CCDC have also been reviewed. The literature examined during the preparation of this work includes all former reviews published by our group [2,3] and by others [4], as well as the succinct annual surveys by Housecroft [5–7].

Technetium chemistry attracts considerable research attention owing to the prominent use of the metastable ^{99m}Tc isomer in diagnostic nuclear medicine [8,9]. The efforts made in this field in recent years have led to the synthesis of new and more efficient radiopharmaceuticals, as described thoroughly in some general [10–14] and specific reports [15,16]. Accordingly, ^{99m}Tc-based agents continue to play a significant role in medicinal inorganic chemistry [17]. Fig. 1 shows some representative ^{99m}Tc agents that have been developed successfully following inorganic chemistry investigations. Six of these molecules are already marketed compounds currently used in everyday practice, whereas the others are under advanced clinical trials.

The total number of structurally characterized technetium compounds in the 1993–1999 period is 196. Fig. 2 correlates the number of X-ray structures with the publication year. The comparison with the data of the previous 7 years reveals that the biggest effort in the crystallographic characterization of Tc complexes was accomplished at the beginning of the 1990s, when advanced perfusion agents were introduced into the radiopharmaceutical market.

The decline in the number of structural investigations at the end of the 1990s likely reflects a target change in the field of radiodiagnostics. In fact, the research

is moving rapidly from purely inorganic complexes towards more complicated entities. This shift is motivated by the need for optimizing the biolocalization of the diagnostic agent. The localization of pure inorganic complexes depends on physico-chemical properties strictly related to the inner metal coordination sphere, such as charge, molecular weight or size. The biolocalization of newer compounds is instead very specific, for it is mainly due to interactions with a receptor or metabolic transformations involving the outer coordination sphere.

In the present study, individual compounds are organized in groups according to a common feature. Within each group, the complexes have been arranged in order

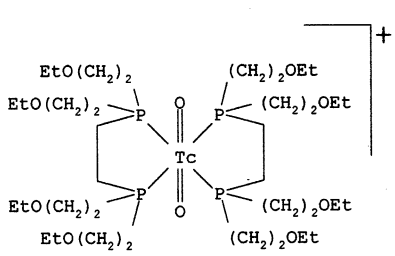

^{99m}Tc-tetrofosmin
Myoview™
Amersham
heart

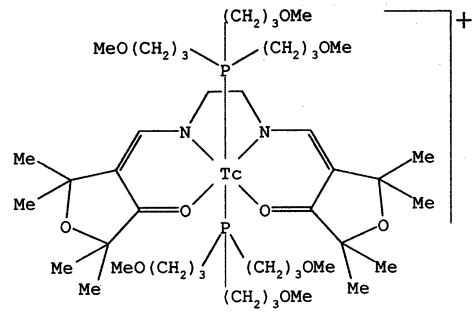

^{99m}Tc-furifosmin
Technescan Q12™
Mallinckrodt
heart

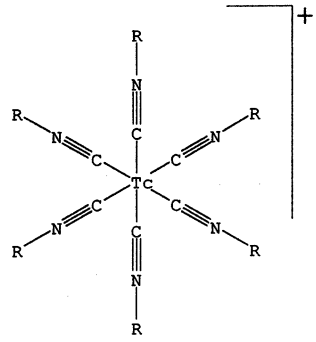

R = $CH_2C(CH_3)_2OCH_3$

^{99m}Tc-sestamibi
Cardiolite™
DuPont
heart

Fig. 1. Selected ^{99m}Tc-radiopharmaceuticals commercially available or under clinical evaluation.

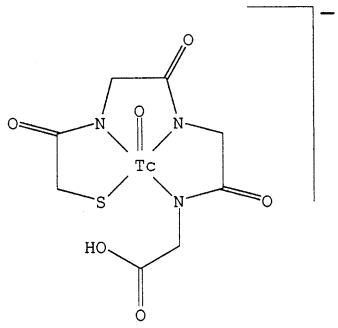

^{99m}Tc-MAG$_3$
Technescan Mag$_3$™
Mallinckrodt
kidney

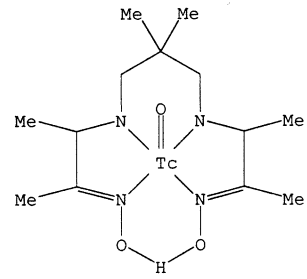

^{99m}-Tc-d,l-HM-PAO
Ceretec™
Amersham
brain

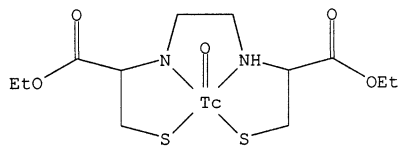

^{99m}Tc-ll-ECD
Neurolite™
DuPont
brain

Fig. 1. (*Continued*)

of increasing coordination number (c.n.) and increasing complexity of the coordination sphere at the metal center. The three main groups include the complexes with metal–nitrogen multiple bonds, the oxo-complexes and the low-valent Tc complexes. These groups are by far the more populated and represent more than 90% of the structures.

In this work, the compounds are numbered according to their reference. If more than one structure is reported in the same paper, as in Ref. [33], where three complexes are described, they are labeled as [33a], [33b] and [33c].

2. Complexes with metal–nitrogen multiple bonds

In this section the complexes containing metal–nitrogen multiple bonds are discussed. Thus, the classic nitrido compounds (Section 2.1) are put together with

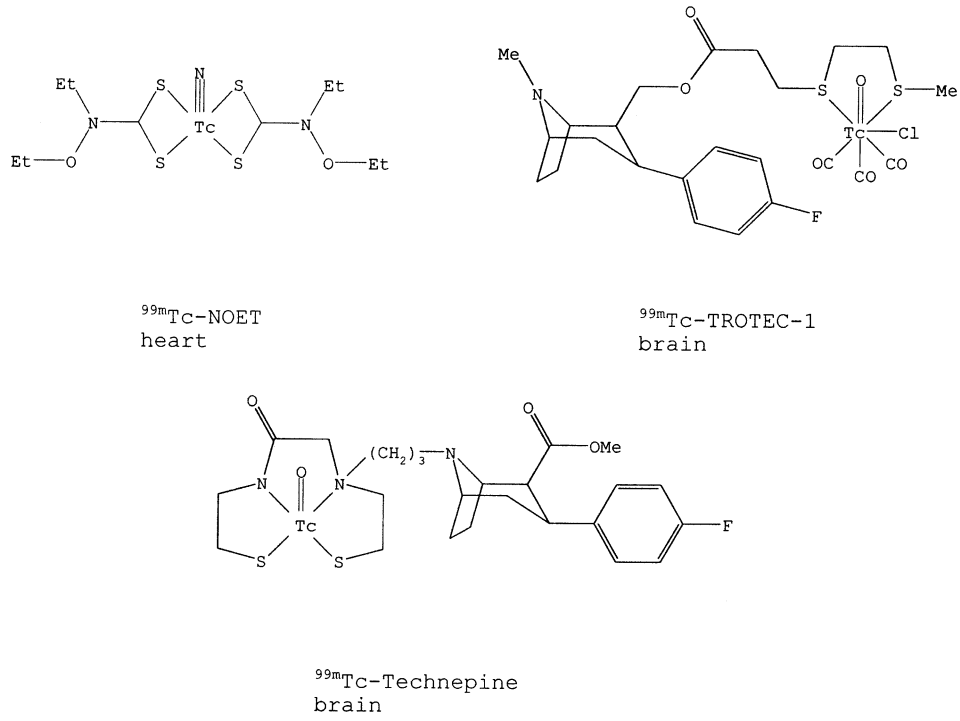

Fig. 1. (*Continued*)

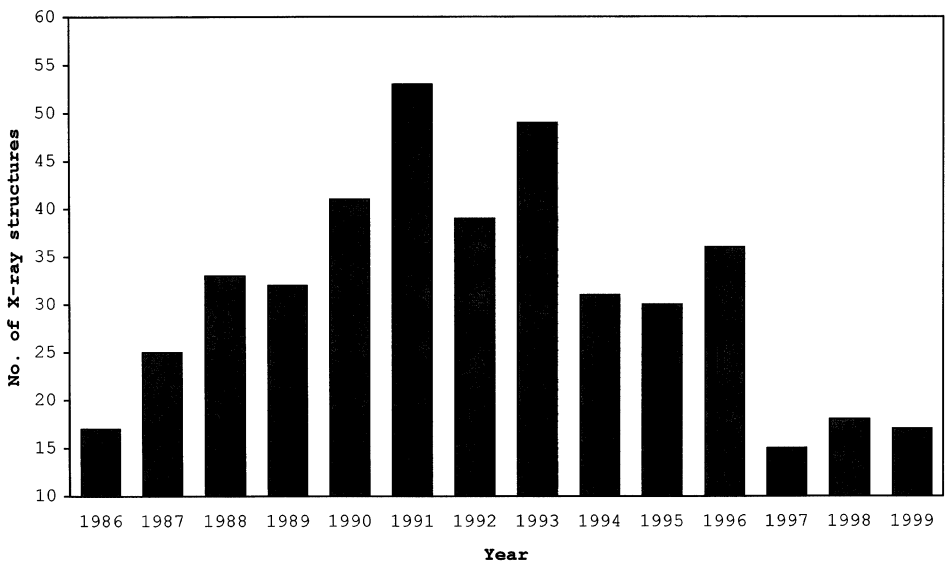

Fig. 2. Number of Tc crystal structures versus year of publication.

the imido species (Section 2.2), the diazenido complexes (Section 2.3) and the less common nitrosyl and thionitrosyl derivatives (Section 2.4). The variety of nitrogen donors dictates the formation of quite different and distinctive cores, where the oxidation number (o.n.) of the metal varies from I to VII. This class of compounds has become increasingly attractive in the last decade because of the introduction of new and efficient methods for producing the nitrido [18] and the hydrazinonicotinamide (HYNIC) [19] cores at the 'no carrier added' level.

2.1. Nitrido–Tc(V) complexes

All these compounds contain the $[Tc{\equiv}N]^{2+}$ core. Some derived structural parameters are summarized in Table 1, where the complexes are divided into two classes according to the symmetry imposed by the ligands. Analysis of the data reveals that five- and six-coordinate species are almost equally represented. Five-coordinate complexes have two ideal limiting geometries: square pyramidal (s.p., $\tau = 0.0$) and trigonal bipyramidal (t.b.p., $\tau = 1.0$). The geometry is characterized by the trigonality index τ first described by Addison et al. [20]. This index is a pure number and it is defined as $(\beta - \alpha)/60$, where α and β are the two largest angles around the Tc atom. Most compounds show a τ value approaching the s.p. arrangement, whereas a few significant examples move towards the t.b.p. array. Usually, π-donors lead to the formation of distorted s.p. species by totally filling the basal plane of the pyramid, with the nitrido group at the apex. On the contrary, a combination of π-donors and π-acceptors promotes the formation of t.b.p. complexes, as shown in Fig. 3.

Five-coordinate species are frequently neutral, the charge of the nitrido moiety being saturated by ionizable thiols, dithiocarbamates or amides, as in $[TcN(HEt_2tcb)_2]$ [26a] ($HEt_2tcb = N,N$-diethyl thiocarbamoylbenzamidinate $(1-)$) and [TcN(eacyd)] [30] (eacyd = N,N'-ethylene-bis-(methyl-2-aminocyclopentane-1-dithiocarboxylate) $(2-)$). However, if only bidentate or tetradentate neutral donors, such as non-ionizable amines, amides or phosphines are present, the c.n. expands to six by addition of a monodentate ligand trans to the nitrido group. The resulting distorted octahedral complexes are mostly cationic. The largest deviation from the ideal octahedron arises from the trans-axial lengthening produced by the nitrido group onto the monodentate ligand. This deformation is evident in the complex $[TcN(pnao)(H_2O)]^+$ [31] (pnao = 3,3,9,9-tetramethyl-4,8-diazaundecane-2,10-dione dioximate $(1-)$), in the pnao-like species $[TcN(bnao)(H_2O)]^+$ [32a] (bnao = 3,3,10,10-tetramethyl-4,9-diazadodecane-2,11-dione dioximate $(1-)$) and $[TcN(pentao)(H_2O)]^+$ [32b] (pentao = 3,3,11,11-tetramethyl-4,10-diazatridecane-2,12-dione dioximate $(1-)$) and in the phosphinoamino complex $[TcNCl(PNH_2)_2]^+$ [28]. Interestingly, the dithiocarbamate ligand of $[TcN(Et_2dtc)_2(PMe_2Ph)]$ [26b] (Fig. 4) is the sole example so far reported showing an axial $[N{\equiv}Tc{-}S]^{2+}$ moiety, as opposed to the more common $[N{\equiv}Tc{-}OH_2]^{2+}$ and $[N{\equiv}Tc{-}Cl]^+$ ones.

Only four donor atoms: S (33.8%), P (28.1%), N (20.1%) and Cl (13.7%) account for more than 95% of the donors. Thus, the chemist willing to synthesize new

Table 1
Some structural parameters for nitrido–Tc(V) complexes

Compound	Donor set	C.n.	τ[a] (°)	N≡Tc–$L_{(trans)}$ (°)	Δ[b,c] (Å)	Ref.
Class (i)						
$[TcN(Smetetraz)_4]^{2-}$	NS_4	5	0.02		0.58	[21a]
$[TcN(dmit)_2)^{2-}$	NS_4	5	0.08		0.62	[22]
$[TcN\{(SPPh_2)_2N\}_2]$	NS_4	5	0.08		0.60	[23a]
$[TcNCl(SCH_2CH_2PCy_2)(PPh_3)]$	NP_2SCl	5	0.28		0.65	[24a]
$[TcN(SCH_2CH_2PPh_2)_2]$	NP_2S_2	5	0.50		0.60 (0.01)	[25a]
$[TcN(SCH_2CH_2CH_2PTol_2)_2]$	NP_2S_2	5	0.81		0.00 (0.00)	[25b]
$[TcN(HEt_2tcb)_2]$	N_3S_2	5	0.07		0.61	[26a]
$[TcNCl(dmpe)_2]^+$	NP_4Cl	6		177.4	0.27	[27a]
$[TcNCl(dppe)_2]^+$	NP_4Cl	6		disorder	0.00	[27b]
$[TcNCl(PNH_2)_2]^+$	N_3P_2Cl	6		179.5	0.26	[28]
$[TcN(Hbiguan)_2(H_2O)]^{2+}$	N_5O	6		177.3	0.44	[29a]
[TcN(eacyd)]	N_3S_2	5	0.02		0.59	[30]
$[TcN(pnao)(H_2O)]^+$	N_5O	6		175.9	0.40	[31]
$[TcN(bnao)(H_2O)]^+$	N_5O	6		175.1	0.34	[32a]
$[TcN(pentao)(H_2O)]^+$	N_5O	6		176.2	0.32	[32b]
$[TcNCl(14S4)]^+$	NS_4Cl	6		176.4	0.24	[33a]
$[TcNCl(18S6)]^+$	NS_4Cl	6		177.4	0.21	[33b]
$[TcNCl(16S4)(OH)_2]^+$	NS_4Cl	6		178.5	0.11	[33c]
Class (ii)						
$[TcNCl_2(PPh_3)_2]$	NP_2Cl_2	5	0.36		0.60	[34]
$[TcNCl_2(PPh_2py–P)_2]$	NP_2Cl_2	5	0.36		0.60	[35]
$[TcN(SCH_2CH_2PCy_2)_2]$	NP_2S_2	5	0.49		0.73(0.00)	[24b]
$[TcN(PMe_2Ph)_2(mnt)]$	NP_2S_2	5	0.00		0.57	[36]
[TcNCl(CYS–OEt)(PPh_3)]	N_2PSCl	5	0.20		0.59	[37]
$[TcNCl_2(PN(Pr)P)]$	NP_2Cl_2/N	5/6[d]	0.11		0.41	[38a]
$[TcNCl_2(POOP)]$	NP_2Cl_2/O	5/6[d]	0.43		0.34	[38b]
$[TcNCl_2(POP)]$	NP_2Cl_2/O	5/6[d]		179.3	0.52	[39]
$[TcNCl(PMe_2Ph)_2\{(SPPh_2)_2N\}]$	NP_2S_2Cl	6		170.5	0.30	[23b]
$[TcN(Et_2dtc)_2(PMe_2Ph)]$	NPS_4	6		161.6	0.42	[26b]
[TcN(*Z*-Val-dtc)(PPh_3)]	N_3PS	5	0.27		0.62	[40a]
$[TcN(POP)(dtc)]^+$	N_2P_2S/O	5/6[d]		159.8	0.48	[41]
$[TcN(PN(etOMe)P)(dtc)]^+$	N_2P_2S/N	5/6[d]		161.8	0.43	[42]

[a] $\tau = (\beta - \alpha)/60$ where α and β are the two largest angles around Tc.

[b] Δ is the displacement of Tc from the basal plane towards the nitrido atom.

[c] The values shown in parentheses indicate the Tc displacement from the basal plane in trigonal bipyramidal geometry.

[d] C.n. intermediate (see text).

ligands suitable for coordination around the $[Tc{\equiv}N]^{2+}$ core needs to test only a restricted domain of the Periodic Table. In s.p. complexes, the displacement of Tc (Δ_{Tc}) from the mean basal plane towards the nitrido atom lies within the 0.58–

0.73 Å range, whereas in six-coordinate species the deviation varies from 0.11 and 0.44 Å. However, some nitrido complexes show Δ_{Tc} values somewhat in between these two ranges. The c.n. of these molecules can be either five or six, and it is not always clearly defined (Table 1).

In such complexes the sixth site trans to the $[Tc{\equiv}N]^{2+}$ group is undoubtedly occupied, but the metal–donor interaction is questionable. With the exception of

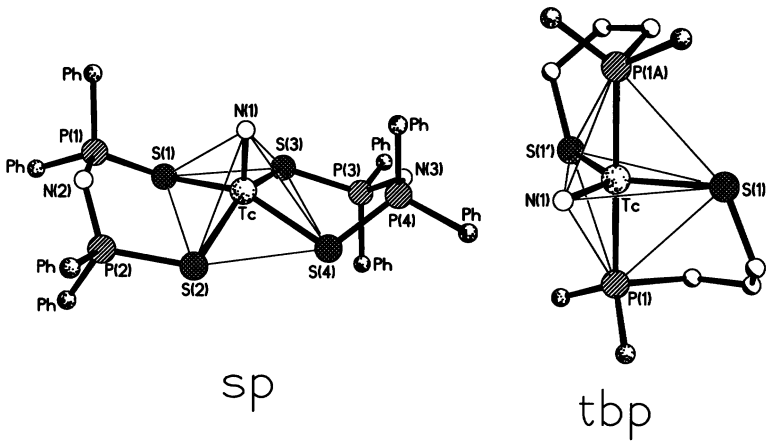

Fig. 3. Square pyramidal versus trigonal bipyramidal geometries in $[TcN\{(SPPh_2)_2N\}_2]$ [23a] ($\tau = 0.08$) and $[TcN(S(CH_2)_3PTol_2)_2]$ [25b] ($\tau = 0.81$).

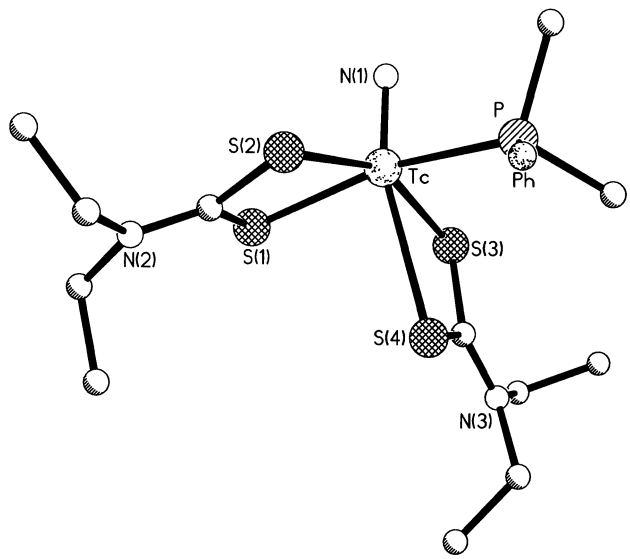

Fig. 4. $[TcN(Et_2dtc)_2(PMe_2Ph)]$ [26b], the only example of a sulfur donor trans to the [Tc≡N] group.

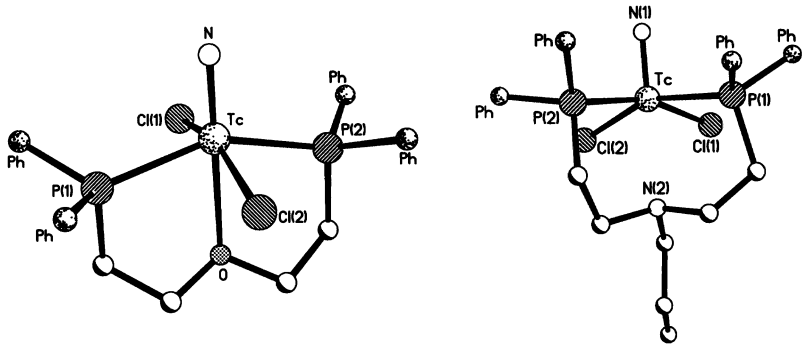

Fig. 5. *mer*-[$TcNCl_2$(POP)] [39] and *fac*-[$TcNCl_2$(PN(Pr)P)] [38a]: the heteroatom in the diphosphine chain dictates the isomer form.

the already-mentioned complex [26b], all these compounds present a diphosphine ligand incorporating at least one heteroatom (X) in the chain between the phosphorus donors (PXP). This feature, coupled with a sufficiently large P···P bite distance, forces monosubstitution of the diphosphine at the $[Tc{\equiv}N]^{2+}$ group, affording neutral species of the type [$TcNCl_2$(PXP)]. Examples include [$TcNCl_2$(PN(Pr)P] [38a], [$TcNCl_2$(POOP)] [38b] and [$TcNCl_2$(POP)] [39].

It is worth noting that the chemical nature of the heteroatom in the diphosphine framework addresses the formation of meridional and/or facial isomers. Thus, etheric oxygen stabilizes *mer*,*trans*-[$TcNCl_2$(POP)] [39] (Fig. 5) and *mer*,*trans*-[$TcNCl_2$(POOP)] [38b], whereas tertiary amino nitrogen affords *fac*-[$TcNCl_2$(PN(Pr)P)] [38a] (Fig. 5).

These monosubstituted species are activated intermediates that easily exchange halides for incoming bidentate ligands, yielding mixed bis-substituted heterocomplexes like $[TcN(POP)(dtc)]^{+}$ [41] and $[TcN(PN(etOMe)P)(dtc)]^{+}$ [42] (Fig. 6). Most importantly, this mixed coordination sphere allows the introduction of biologically active fragments in nitrido-containing species, an approach that has been elusive in the past.

There is only one nitrido complex where Tc has an o.n. higher than V, namely the octahedral *mer*-[$TcNCl_3$(bpy)] [43]. The major feature of this molecule is the lengthening by 0.24 Å of the Tc–N_{bpy} distance trans to the nitrido atom with respect to the other Tc–N_{bpy} bond. Finally, we note [$\{TcN(thiourea)\}_4(edta)_2]\cdot 6H_2O$ [44], the sole example of a polynuclear nitrido–Tc(V) complex. This compound adopts a cyclic tetrameric [Tc_4N_4] configuration with four asymmetric [Tc≡N–Tc] bridges.

2.2. Imido complexes

The imido ligand (NR^{2-}) is known to stabilize high formal o.ns. In fact, this section includes Tc(VII), Tc(VI) and Tc(V) imido complexes. The repeated π-loading provided by additional bulky imido groups induces the formation of four-coor-

dinate tetrahedral Tc(VII) complexes, such as [Tc($N^{isopr}Ar)_3$Me] [45] (Fig. 7), [Tc($N^{isopr}Ar)_3(OSiMe_3)$] [46a] and [Tc($N^{isopr}Ar)_3$I] [46b].

The multiple-bonded Tc–N mean distance in these species is 1.750(8) Å, and the Tc–N–C angle ranges from 155.8(6)° in [46a] to 166.6(6)° in [46b]. In fact, even if bent and linear imido coordination modes are generally taken into account to assess the M–N bond order, the relationship between M–N bond lengths and M–N–C angles is not so clear, as also indicated by theoretical calculations [45].

Reduction of the iodo compound with elemental sodium yields the Tc(VI) ethane-like dimer [$Tc_2(N^{isopr}Ar)_6$] [47]. In the latter, each Tc atom is bound to three symmetry-equivalent imido ligands positioned in a staggered arrangement, and the

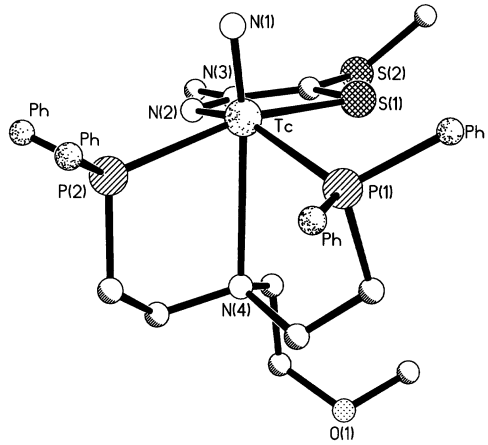

Fig. 6. The [TcN(dtc)(PN(EtOMe)P)]$^+$ heterocomplex [42].

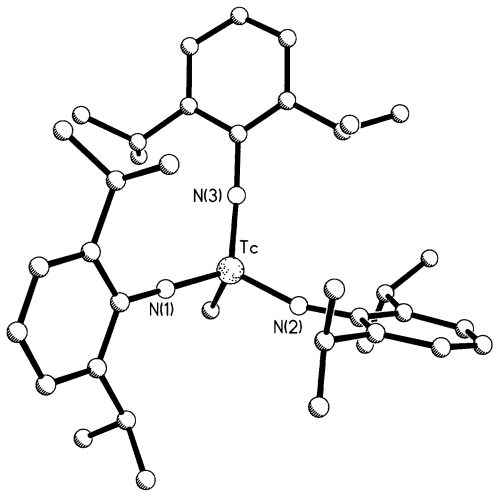

Fig. 7. The tetrahedral complex [Tc($N^{isopr}Ar)_3$Me] [45].

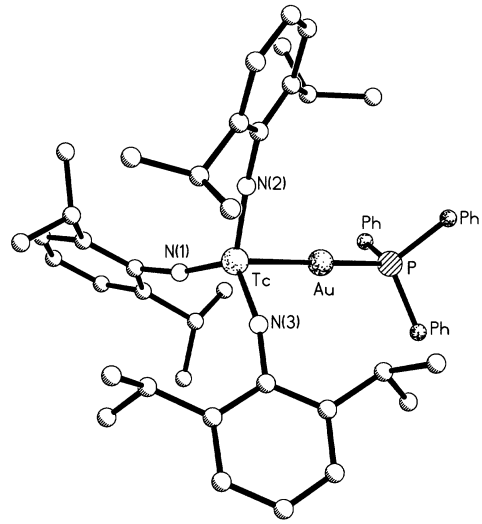

Fig. 8. The heterometallic complex $[Tc(N^{isopr}Ar)_3Au(PPh_3)]$ [48b].

Tc–Tc bond length is 2.744(1) Å. The use of less-crowded imido groups affords the 'edge-bridged' tetrahedral Tc(VI) dimer $[Tc_2(N^{Me}Ar)_4(\mu\text{-}N^{Me}Ar)_2]$ [48a] containing four terminal and two μ-bridged arylimido units with a Tc–Tc distance of 2.696(2) Å. The formation of ethane-like or 'edge-bridged' species appears to be determined only by steric factors, as complexes [47] and [48a] can be considered isoelectronic.

Stepwise reaction of 'edge-bridged' [48a] with a methyl Grignard reagent results in displacement of successive terminal imido groups and in the formation of $[TcMe_2(N^{Me}Ar)_2(\mu\text{-}N^{Me}Ar)_2Tc(N^{Me}Ar)_2]$ [49a] and $[\{TcMe_2(N^{Me}Ar)(\mu\text{-}N^{Me}Ar)_2\}_2]$ [49b]. Sodium reduction of [48a] affords instead the tri-coordinate $[Tc(N^{isopr}Ar)_3]^-$ nucleophile. This intermediate species reacts with electrophilic metallic fragments to give the heteronuclear Tc(V) species $[Tc(N^{isopr}Ar)_3Au(PPh_3)]$ [48b] (Fig. 8) and $[\{Tc(N^{isopr}Ar)_3\}_2Hg]$ [48c], which represent the first examples of Tc–Au and Tc–Hg bonds (2.589(1) Å and 2.615(1) Å respectively).

The geometry of both compounds can be described as a distorted trigonal-based pyramid with the heteronucleus at the apex. Interestingly, the $[Tc(NAr)_3]^-$ fragments in [48b] and [48c] are almost identical, showing no effect of the metal cation.

On the other hand, the coordination of only one imido unit produces the $[TcNR]^{3+}$ core that is isoelectronic with the $[TcO]^{3+}$ moiety. Three crystal structures of phenylimido–Tc(V) species have recently been determined: $[Tc(NPh)Cl_2(PMe_2Ph)_3]^+$ [50], $[Tc(NPh)Cl_3(PMePh_2)_2]$ [51a] and $[Tc(NPh)Br_3(PMePh_2)_2]$ [51b]. By replacing the bulky $PMePh_2$ with the less encumbered PMe_2Ph, neutral complexes of the type $[Tc(NPh)X_3(PMePh)_2]$ rearrange to the cationic species $[Tc(NPh)X_2(PMe_2Ph)_3]^+$, retaining the 18-electron valence configuration. In these complexes, the absence of the steric constraints imposed by polydentate ligands leads to a slight distortion of the ideal octahedron. In fact, the Tc atom

moves off the mean basal plane towards the imido unit by only 0.11(2) Å; the mean Tc–N length is 1.706(5) Å and the mean Tc–N–C angle is 175.7(3)°. These data confirm the linear mode of the multiple-bonded phenylimido unit.

In these compounds the coordination sphere is always filled by monodentate co-ligands. However, the introduction of polydentate ligands into this flexible core might allow the design of a new class of radiopharmaceuticals able to reproduce, to some extent, the rich chemistry of the isoelectronic $[TcO]^{3+}$ core bearing chelate frameworks.

2.3. Diazenido complexes

The chemistry of diazenido compounds appears to be much more challenging. Since the introduction of the 'HYNIC' approach in the early 1990s [19], interest in this area has rapidly grown, with the ultimate goal of clarifying the molecular structure of diazenido-containing agents. To the best of our knowledge, crystallographic analysis of HYNIC-based agents has not yet provided certainty about configuration. However, investigation of some model compounds has laid the basis for understanding their molecular identity. Thus, studies on Tc complexes bearing the hydrazinopyridine ligand have established the formation of the robust [Tc=NNR] moiety and have also disclosed the possibility for chelate formation through the pyridine nitrogen.

Table 2 reports the eight crystal structures solved in the past 7 years. Seven complexes are six-coordinate, and one is the five-coordinate diamagnetic t.b.p. species $[TcCl(N{=}NPhCl)_2(PPh_3)_2]$ [53a] containing two linear diazenido groups (Fig. 9). In this case the strong donating property of the diazenido units (formally $3e^-$ donors) (Scheme 1) supplies enough electron density for a closed electron shell, thereby preventing six coordination.

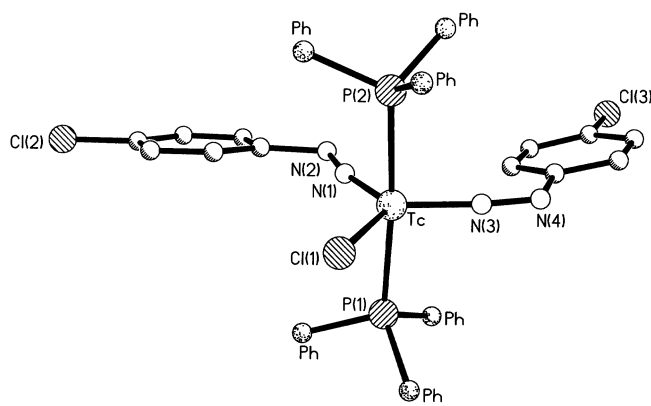

Fig. 9. Five-coordinate $[TcCl(N{=}NPhCl)_2(PPh_3)_2]$ [53a] containing two linear diazenido groups.

Table 2
Some structural parameters for diazenido–Tc complexes

Compound	Donor set	C.n.	Tc–N(1) η_1-mode (Å)	N(1)–N(2) (Å)	Tc–N(1–N(2) (°)	N(1)–Tc–$L_{(trans)}$ (°)	Δ[a] (Å)	Tc–N(3) η_2-mode (Å)	Ref.
$[TcCl_3(N{=}NPh_2)(PPh_3)_2]$	NP_2Cl_3	6	1.738(4)	1.300(5)	175.6(3)	177.4(1)	0.11		[52]
$[TcCl(N{=}NPhCl)_2(PPh_3)_2]$	N_2P_2Cl	5	1.78(1)	1.25(3)	166(1)		0.01 (0.94)[b]		[53a]
$[TcCl(N{=}NPh)(dppe)_2]^+$	NP_4Cl	6	1.92(2)[c]	1.25(4)	163(2)	177.3(6)	0.00		[53b]
$[TcBr_2(N{=}NPh)(PMe_2Ph)_3]$	NP_3Br_2	6	1.77(1)	1.21(2)	172(1)	172.9(4)	0.09		[51c]
[Tc(salen)-(N=NPhCl)(PPh_3)]	N_3O_2P	6	1.764(8)	1.24(1)	173.6(7)	176.0(3)	0.11		[54]
$[Tc(SPh)_2$-(N=Npy)(HN=Npy–N)$]_2$	N_3S_3	6	1.78(1)	1.24(1)	174.2(8)	162.0(4)	0.22		[55]
[Tc(Spy)(N=Npy)(Spy–N)-(HN=Npy–N)]	N_4S_2	6	1.767(9)	1.24(1)	175.1(8)	164.0(4)	0.23	2.015(8)	[56]
mer-$[Tc(CO)_3$-(HN=NPh-*t*-bu)$(PPh_3)_2]^+$	C_3NP_2	6	2.157(6)	1.243(8)	124.2(5)	178.0(3)	0.05[d]	1.985(9)	[57]

[a] Δ is the displacement of Tc from the basal plane towards N(1).
[b] The τ index is reported in parentheses.
[c] Abnormally long.
[d] Far from N(1).

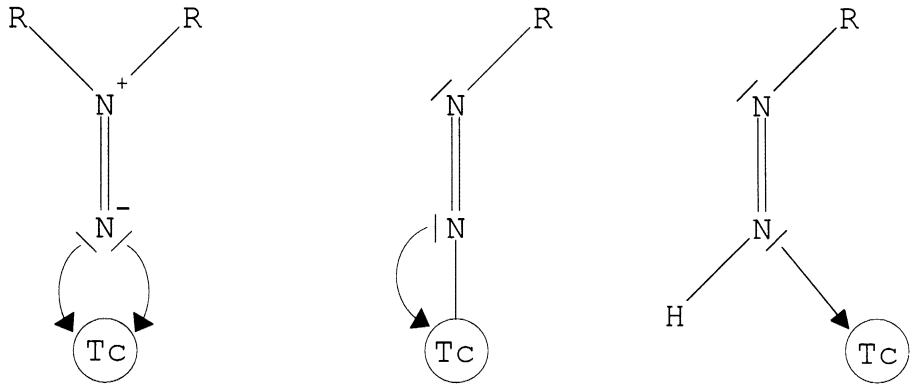

linear isodiazene
neutral, 4 e⁻ donor

linear diazenido
mononegative, 3 e⁻ donor

bent diazenido
neutral, 2 e⁻ donor

Scheme 1.

As usual, the two phosphorus atoms of the π-acceptor phosphines occupy the apices of the bipyramid, while the π-donors (bis-diazenido and halide) are at the triangular base. In $[TcBr_2(N{=}NPh)(PMe_2Ph)_3]$ [51c], $[TcCl(N{=}NphCl)_2(PPh_3)_2]$ [53a], $[TcCl(N{=}NPh)(dppe)_2]^+$ [53b] and [Tc(salen)(N=NPhCl)(PPh_3)] [54] the diazenido group coordinates as a mononegative η^1-ligand, with halides and/or phosphines consistently participating in the coordination sphere. Owing to the mononegative charge of the linear diazenido group, the metal is formally Tc(III), with a low-spin d^4 configuration, consistent with the observation of sharp ^{1}H- and ^{31}P-NMR signals typical of diamagnetic compounds [53,54]. The diazenido group induces no significant trans influence. Likewise, the zwitterionic $[N{=}NPh_2]$ isodiazene ligand, which acts as a neutral $4e^-$ donor (Scheme 1) in *mer*,*trans*-$[TcCl_3(N{=}NPh_2)(PPh_3)_2]$ [52], does not exert any trans influence.

The introduction of thiolate ligands in diazenido compounds leads to more complex species. Aromatic benzenethiolate gives the dimer species $[Tc(SPh)_2(N{=}Npy)(HN{=}Npy{-}N)]_2$ [55], in which both thiolates bridge the metal centers and the hydrazinopyridine group coordinates to the metal using both η^1 and η^2 modes. These demonstrate the linear [Tc–N–N] stick and the characteristic bent [Tc–N–N] unit. The 2-pyridinethiolate ligand affords the even more complex monomer [Tc(Spy)(N=Npy)(Spy–N)(HN=Npy–N)] [56] (Fig. 10), which shows a rare combination of the η^1 and η^2 coordination modes of both the pyridinethiolate and pyridinediazenido ligands. The relevant metal–nitrogen bonds are 1.767(9) Å, 1.985(9) Å, 2.150(7) Å and 2.144(9) Å for linear Tc–N – N hydrazinopyridine, bent Tc–N–N hydrazinopyridine, Tc–N pyridinehydrazino and Tc–N 2-pyridinethiolato respectively.

The bent diazenido moiety also appears in *mer*-$[Tc(CO)_3(HN{=}NPh\text{-}t\text{-}bu)(PPh_3)_2]^+$ [57] (Fig. 11). In this case, the Tc–N bond lengthening (2.157(6) Å) does not arise from any chelating effect imposed by the diazene group. On the contrary, both the electron-rich Tc(I) metal center and the tricarbonyl co-ligands seem to play a role in preventing multiple Tc–nitrogen interactions. It is also worth noting the meridional coordination of the carbonyl groups, as opposed to the more common facial coordination (Section 4.3).

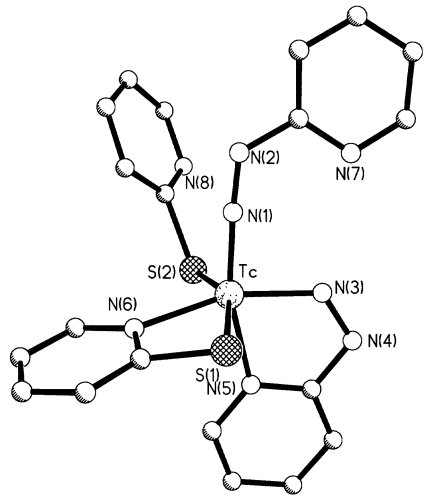

Fig. 10. High complexity degree in the [Tc(Spy)(N=Npy)(Spy–N)(HN=Npy–N)] species [56], with η^1 and η^2 coordination modes of both ligands.

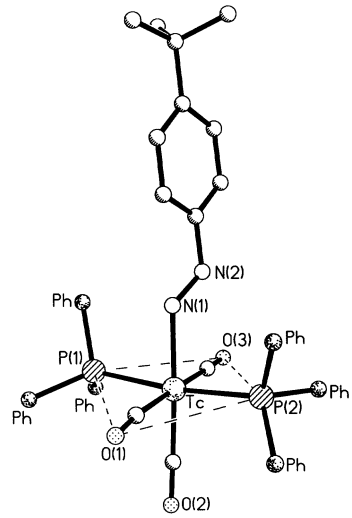

Fig. 11. The unique *mer*-$[Tc(CO)_3(HN{=}NPh\text{-}t\text{-}bu)(PPh_3)_2]^+$ cation [57].

2.4. Nitrosyl and thionitrosyl complexes

This section includes four crystal structure determinations of nitrosyl–Tc(I) complexes and a fifth one describing a thionitrosyl–Tc(II) species. The mixed η^2-diazenido nitrosyl complex $[Tc(NO)Cl_2(HN{=}NPy)(PPh_3)]$ [58] provides a sort of connection with Section 2.3. In this molecule the N-based bent diazenido (Tc–N–N angle of 126.2 (3)°), hydrazinopyridine and nitrosyl groups are coordinated in a meridional fashion. Owing to the cationic nature of the nitrosyl donor, this compound and the other nitrosyl complexes $[Tc(NO)Cl(DIARS)_2]^+$ [59], $[Tc(NO)Cl_2(pyPPh_2–P,N)(pyPPh_2–P)]$ [60] and *mer*-$[Tc(NO)Cl_2(py)_3]$ [61] are electron-rich Tc(I) diamagnetic compounds. The overall coordination about Tc is close to octahedral. The displacement of Tc from the mean basal plane averages 0.10 Å and the mean value of the Tc–N–O angle is 176.1(4)°. In [59] and [61] the NO and the trans-Cl ligands exhibit twofold disorder, so preventing the differentiation of the two groups. π-Acceptor donors, such as phosphines, arsines and/or pyridines, usually complete the coordination sphere, and there is an open competition between phosphines and pyridines. Thus, PPh_3 is displaced by incoming pyridine, as demonstrated by ligand-exchange reactions onto the labile $[Tc(NO)Cl_2(PPh_3)(NCMe)]$ to promote the formation o f $[Tc(NO)Cl_2(py)_3]$ [61]. On the contrary, the use of the potentially bidentate phosphinopyridine ligand affords $[Tc(NO)Cl_2(pyPPh–P,N)(pyPPh_2–P)]$ [60], in which the challenge awards phosphorus over nitrogen.

In the thionitrosyl complex $[Tc(NS)Cl_3(PMe_2Ph)_2]$ [23c] the $[TcNS]^{3+}$ core is almost linear with a bond angle of 176.2(3)°, and the bonding mode of the thionitrosyl group is NS^+, with extensive back-bonding to Tc(II). Accordingly, the pertinent Tc–Cl distance lengthens to 2.432(1) Å. Unlike the other compounds of this series, complex [23c] is paramagnetic, as established by EPR spectroscopy. As already observed for imido–Tc(V) complexes, the use of ligands of greater denticity might introduce one to a class of more stable low-valent nitrosyl and thionitrosyl species.

3. Oxo-complexes

This section describes two groups of compounds: classical mono-oxo Tc(V) species (37 entries) and less common di-oxo and μ-oxo complexes showing the characteristic $[Tc^VO_2]^+$ and $[Tc_2^VO_3]^{4+}$ or $[Tc_2^{III}O]^{4+}$ cores respectively (11 complexes). The first group is divided in turn into including (i) complexes with three sub-groups, tetradentate ligands, (ii) compounds belonging to the so-called '3 + 1' system and (iii) various structures that do not fit into the above classification.

Oxo–Tc(V) species containing polydentate ligands have marked a milestone in the development of radiopharmaceuticals, as Fig. 1 illustrates. The chemistry of these compounds is still widely investigated because of the possibility of introducing bio-fragments onto the chelate framework [11–14].

3.1. Mono-oxo Tc(V) complexes

As in previously observed nitrido Tc(V) complexes, the presence of the distinctive mono-oxo Tc(V) moiety determines the donor set type. In more than 90% of the cases, the coordination sites are occupied by only three types of atom, i.e. N (37.7%), O (27.5%) and S (25.5%). Ligands with high denticity (tridentate and tetradentate) lead to the formation of five-coordinate complexes, owing to the steric requirements imposed by the chelate framework. There are only two exceptions, [TcO(EC)] [67] (EC = *N*,*N*′-bis-1-(carboxy-2-mercaptoethyl)ethylenediaminate (3−) and [TcO(dppd)(OMe)] [74], in which the c.n. reaches six. By contrast, bidentate ligands induce the formation of distorted octahedral geometries, the sole exception being represented by the complex $[TcO(biguan)_2]^+$ [29b]. The latter is also the sole cationic species of the series.

Neutral compounds (75.6%) are largely favored, whereas the well-known MAG_3-type species are anionic (Table 3).

In five-coordinate complexes the Tc atom is displaced from the mean basal plane toward the oxo-oxygen and the displacement varies between 0.62 Å in [TcO(AADT)–N–(3-chloropropyl)] [63b] and 0.84 Å in $[TcO(CTA)]^-$ [71]. In six-coordinate complexes, such a displacement ranges between 0.13 Å in $[TcOCl_2(hdto)]$ [80a] and 0.48 Å in [TcO(EC)] [67].

3.1.1. Complexes with tetradentate ligands

Neutral and negatively charged oxo–Tc(V) complexes surrounded by tetradentate ligands have provided the basic framework for the development of technetium-based brain perfusion agents and renal imaging agents. Looking for additional neutral and lipophilic species able to cross the blood brain barrier (BBB), seven mono-oxo complexes have been structurally characterized in the period reviewed. They all contain a tetradentate ligand with two terminal ionizable thiol groups and a combination of amines and amides donors amenable to deprotonation in order to achieve a neutral complex of the type $[TcO(N_2S_2)]$.

Derivatization with phenylpiperidine at the carbon chain linking the two secondary amine groups leads to the formation of syn and anti isomers, depending on the relative orientation of this fragment with respect to the [Tc=O] moiety, as shown by the pair *syn*-[TcO(BAT-PPP)] [62a] and *anti*-[TcO(BAT-PPP)] [62b]. The two forms have different biodistribution properties, the syn-isomer crossing the BBB to a larger extent than the corresponding anti-isomer. It should be stressed that only one amine group loses its proton, while the hydrogen of the second amine is found to be syn to the oxo oxygen in both isomers.

The incorporation of a phenyl group in the propyl chain between the amine nitrogen atoms yields an asymmetric N_2S_2 chelating framework containing two amine groups of different ionizability. As expected, single deprotonation occurs at one of the amine groups leading to neutral [TcOCl(U-BAT)] [64a] (U-BAT = *N*,*N*′-bis[2-mercapto-2-methylpropyl]-2-aminobenzylaminate (3−)) as the major species. An additional 'oxidized' complex, [TcOCl(OU-BAT)] [64b] (OU-BAT = 1,1′,9,9′-tetramethyl-4,5-phenyl-3,-7-diazanonan-1,9-dithiolate (oxidized form) (3−)), is also

Table 3
Some structural parameters for mono-oxo–Tc(V) complexes

Compound	Donor set	C.n.	τ [a] (°)	O=Tc–$L_{(trans)}$ (°)	Δ [b,c] (Å)	Ref.
(i) Section 3.1.1						
syn-[TcO(BAT-PPP)]	N_2OS_2	5	0.42		0.76 (0.06)	[62a]
anti-[TcO(-PPP)]	N_2OS_2	5	0.36		0.77 (0.06)	[62b]
[TcO(AADT)–N–EtAc]	N_2OS_2	5	0.43		0.77 (0.06)	[63a]
[TcO(AADT)–N–(3-chloropropyl)]	N_2OS_2	5	0.36		0.62 (0.05)	[63b]
[TcOCl(U-BAT)]	N_2OS_2	5	0.07		0.70	[64a]
[TcO(OU-BAT)]	N_2OS_2	5	0.16		0.70	[64b]
[TcO(N_2S_2thiaz)]	N_2OS_2	5	0.26		0.73	[65]
[TcO(N_2S_2DADS)]$^-$	N_2OS_2	5	0.05		0.77	[66]
[TcO(EC)]	$N_2O_2S_2$	6		165.1	0.48	[67]
[TcO(MAG_2)]$^-$	N_2OS_2	5	0.10		0.75	[68]
[TcO(MAG_3)]$^-$	N_3OS	5	0.02		0.74	[69a]
[TcO(MAG_3OMe)]$^-$ [d]	N_3OS	5	0.06		0.75	[69b]
[TcO(MAG_3OMe)]$^-$ [e]	N_3OS	5	0.05		0.76	[69c]
[TcO(MAAG)]$^-$	N_3OS	5	0.07		0.76	[70]
[TcO(CTA)]$^-$	N_4O	5	0.23		0.84	[71]
[TcO(CB–PAO)]	N_4O	5	0.02		0.68	[72]
[TcO($PnAONO_2$)]	N_4O	5	0.08		0.65	[73]
[TcO(dppd)(OMe)]	$N_2O_2P_2$	6		155.2	0.31	[74]
(ii) Section 3.1.2						
[TcOCl{SN(etSEt)S}]	NOS_2Cl	5	0.68		0.76 (0.05)	[75a]
[TcOCl(*Z*-Ala-dtc)]	N_2OSCl	5	0.04		0.76	[40b]
[TcO{SN($etNEt_2$)S}(SPhBr)]	NOS_3	5	0.61		0.78 (0.06)	[76a]
[TcO{SN($etNEt_2$)S}(STol)]	NOS_3	5	0.62		0.77 (0.08)	[76b]
[TcO{SN($etNEt_2$)S}(Sbz)]	NOS_3	5	0.61		0.78 (0.07)	[76c]
anti-[TcO{SN($etNEt_2$)S}-(SPhOMe)]	NOS_3	5	0.05		0.74	[76d]
[TcO{SN(etmorph)S}(Sbz)]	NOS_3	5	0.42		0.75 (0.06)	[77]
[TcO{SNN(pyr)}(STol)]	N_2OS_2	5	0.21		0.69	[78a]
[TcO{SNN(pip)}(Sbz)]	N_2OS_2	5	0.25		0.68	[78b]
(iii) Section 3.1.3						
[TcOCl_3(malt)]$^-$	O_3Cl_3	6		162.3	0.19	[79]
[TcOCl_2(hdto)]	$O_2S_2Cl_2$	6		163.5	0.13	[80a]
[TcOCl($OCH_2Py)_2$]	N_2O_3Cl	6		158.7	0.18	[81a]
[TcOCl($OCH_2PyCH_2OH)_2$]	N_2O_3Cl	6		159.6	0.20	[81b]
[TcOBr($OCH_2PyCH_2OH)_2$]	N_2O_3Br	6		158.9	0.20	[81c]
[TcOCl($thoz)_2$]	N_2O_3Cl	6		163.7	0.19	[82]
[TcOCl$(PO)_2$]	O_3P_2Cl	6		164.5	0.29	[83]
[TcO($biguan)_2$]$^+$	N_4O	5	0.17		0.68	[29b]
[TcO$(PNH)_2$(OMe)]	$N_2O_2P_2$	6		158.3	0.22	[84]
[TcO(HAF)(PAC)]	$N_2O_2S_2$	6		156.8	0.22	[85]

[a] τ as in Table 1.
[b] Δ is the displacement of Tc from the basal plane towards the oxo atom.
[c] The values shown in parentheses indicate the Tc displacement from the basal plane in trigonal bipyramidal geometry.
[d] Polymorph 1.
[e] Polymorph 2.

obtained due to a reversible ligand-based redox reaction through the interconversion of the coordinated amino to the coordinated imino group.

Asymmetric N_2S_2 ligands can also be synthesized by direct monoalkylation of a bis-amino bis-protected thiol, thereby generating a class of suitable chelating agents for the $[TcO]^{3+}$ core. The reaction again produces a mixture of syn and anti isomers, as demonstrated by [TcO(AADT)–N–EtAc] [63a] (AADT–N–EtAc = N–(2 - ethylacetate)–N–[2 - (2 - ((S–(tri - phenylmethyl)thio)ethyl)amino)acetyl]–S–(triphenylmethyl)-2-aminoethanethiolate (3 −)) and [TcO(AADT)–N–(3-chloropropyl)] [63b] (AADT–N–(3-chloropropyl) = N–(3-chloropropyl)–N–[2-(2-((S–(triphenylmethyl)thio)ethyl)amino)acetyl]–S–(triphenylmethyl) - 2 - aminoethanethiolate (3 −)). Attempts to increase the denticity of these tetradentate ligands by the introduction of a mercaptoethyl substituent at one amine function do not modify the usual bis-thiolate, amine, amide coordination at the metal center. However, an intramolecular cyclization of the additional mercaptoethyl group takes place to give a thiazolidine ring [TcO(N_2S_2thiaz)] [65] (N_2S_2thiaz = 2-(1′-methyl-1′-mercaptoethyl)-3-(5″-methyl-5″-mercapto-3″-(dehydroaza)hexyl)-thiazolidine (3 −)).

Two more oxo–Tc(V) compounds carrying the well-studied N_4-propylene amine oxime backbone have recently been reported. In [TcO(CB-PAO)] [72] (CB-PAO = 4,8-diaza-3,9-dimethyl-6,6-trimethyleneundecane-2,10-dione dioximate (3 −)) a cyclobutane ring has been incorporated into the ligand framework. The modification increases the lipophilicity and the in vivo stability of the species in order to cross the BBB intact. The similar complex [TcO($PnAONO_2$)] [73] ($PnAONO_2$ = 3,3,9,9-tetramethyl-1-(2-nitro-1H-imidazol-1-yl-9-4,8-diazaundecane-2,10-dione dioximate (3 −)) (Fig. 12) presents a pendant nitroimidazole group susceptible to reduction in vivo. The latter has been introduced in the N_4-chelating system for the detection of hypoxic tissues.

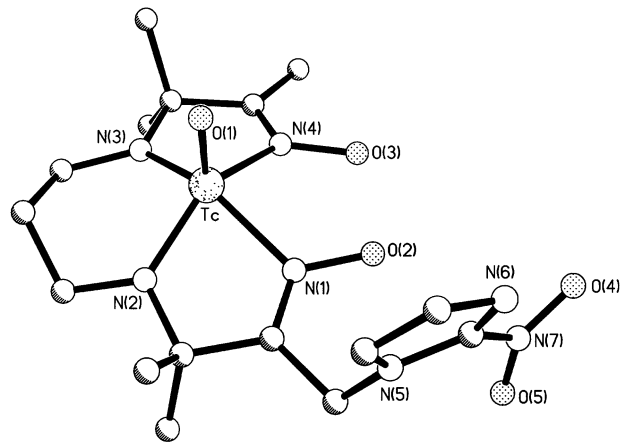

Fig. 12. In [TcO($PnAONO_2$)] [73] the insertion of the nitroimidazole pendant group onto the N_4-framework switches the target organ from the brain to the hypoxic tissue.

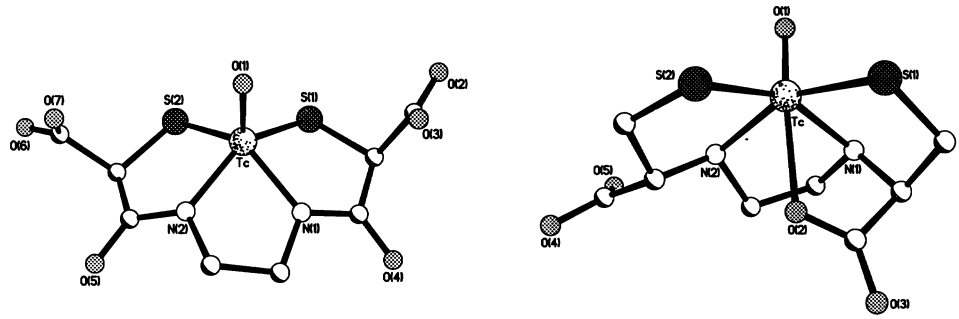

Fig. 13. Five- and six-coordinate complexes $[TcO(N_2S_2DADS)]^-$ [66] and [TcO(EC)] [67]. The hybridization of the N donors allows (or prevents) the coordination of a carboxylate function.

Replacing amine for amide in N_2S_2-tetradentate ligands allows complete deprotonation of both thiol and amide groups to yield negatively charged five-coordinate oxo–Tc(V) compounds, which are used for kidney imaging. The introduction of two symmetrical carboxylate groups on the carbon atoms adjacent to the sulfur atom on the chelate ring gives the expected N_2S_2-type complex $[TcO(N_2S_2DADS)]^-$ [66] (Fig. 13), where the carboxylate groups are not involved in coordination, at least in the solid state.

The contemporary presence of thiols, amides and carboxylic functions in the same chelate can produce different coordination spheres, as found in [TcO(EC)] [67], in which six-coordination is achieved by ligating a carboxylate group trans to the [Tc=O] moiety (Fig. 13). The amide functions are not deprotonated and the two ionizable thiolate donors warrant neutrality to the complex.

The gold standard for kidney imaging is the anionic oxo–Tc(V) agent ^{99m}Tc–MAG_3. The molecular structure of this compound [69a] has recently been elucidated (Fig. 14), along with those of the polymorphous methyl ester derivatives $[TcO(MAG_3OMe)]^-$ [69b,c].

Coordination around the $[TcO]^{3+}$ core is provided by the SN_3 donor set, including a thiolate sulfur and three deprotonated amide nitrogen atoms. This set shapes into the common square pyramid, with the oxo group at the apex and the carboxylic function (or its methyl ester) dangling outside the coordination sphere. Substitution of the central glycine residue with an alanine in the MAG_3 backbone allows isolation of syn-$[TcO(MAAG)]^-$ [70], with no change in coordination. Complete substitution of the glycyl moieties for alanyl fragments affords instead the N_4-tetraalanine ligand, which upon complexation with Tc yields the mono-oxo Tc(V) species of cyclic alanine $[TcO(CTA)]^-$ [71] (Fig. 15).

Four deprotonated amide nitrogen atoms coordinate on the basal plane with all the four methyl groups syn-oriented with respect to the oxo oxygen. By removing one glycyl fragment from the MAG_3 framework, the coordination ability of the resulting mercapto acetyl diglycine (MAG_3) ligand toward the $[TcO]^{3+}$ moiety is significantly affected. The terminal carboxylate group becomes engaged in coordination, providing an SN_2O donor set (Fig. 14) [68] in place of the SN_3 one granted

by the MAG_3 chelate. A rather different tetradentate ligand is found in the six-coordinate neutral compound [TcO(dppd)(OMe)] [74] (dppd = *N*,*N*′-bis[(2-diphenylphosphino)phenyl]propane-1,3-diaminate (2 −)). Here, the uncommon P_2N_2-phosphinoamine chelate ligates on the equatorial plane via two deprotonated amine groups. The complex neutrality is retained by coordination of a methoxide residue trans to the Tc=O linkage.

3.1.2. The '3 + 1' approach

The '3 + 1' mixed-ligand concept has proved to be a successful approach to the preparation of different neutral oxo–technetium complexes. Some of these molecules might find application in radiopharmacy as brain perfusion agents because they are neutral, lipophilic entities able to cross the BBB. The '3 + 1' term highlights the modification occurring in the coordination sphere around the [Tc=O]

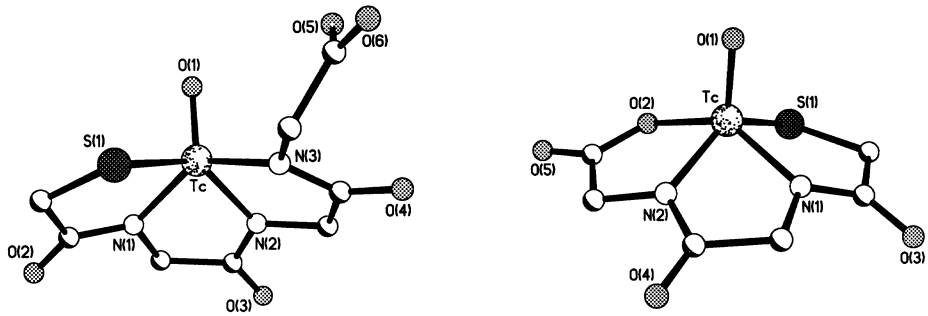

Fig. 14. N_3S–[TcO(MAG_3)]$^-$ [69a] versus N_2SO–[TcO(MAG_2)]$^-$ [68]. In the former, the carboxylic group may bind in a covalent manner to biofragments, in the center; in the latter it is coordinated to the metal center.

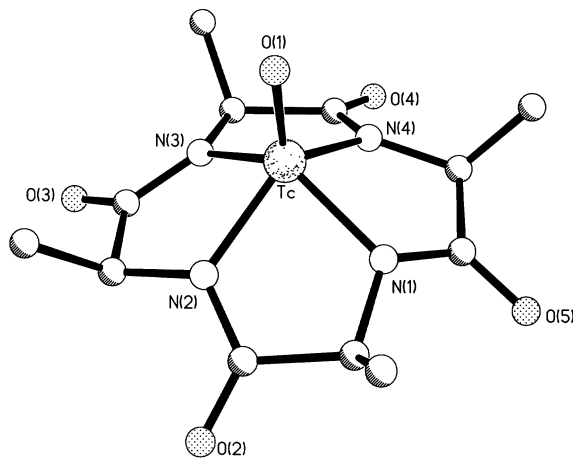

Fig. 15. [TcO(CTA)]$^-$ [71]: cyclization of the tetraalanine peptide.

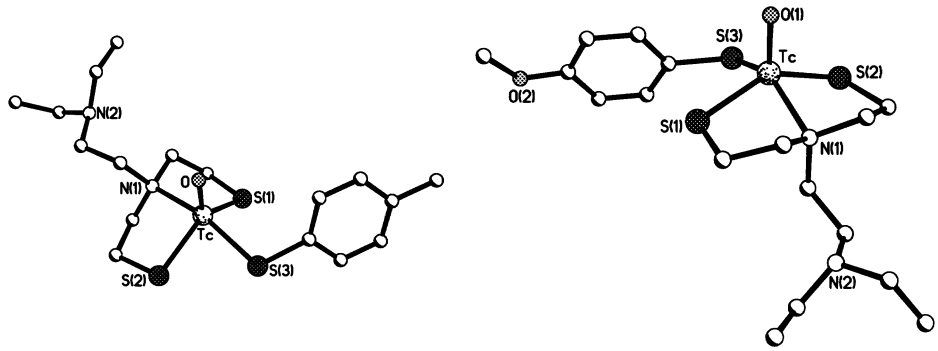

Fig. 16. *syn*-[TcO{SN(etNEt$_2$)S}(STol)] [76b] ($\tau = 0.62$) and *anti*-[TcO{SN(etNEt$_2$)S}(SPhOMe)] [76d] ($\tau = 0.05$). The geometry is determined by the relative orientation of the amine pendant group.

core, where a tetradentate ligand is replaced by a combination of a tridentate plus a monodentate donor (usually a thiol). The change in the coordination environment brings an increased flexibility to the system, and, in fact, the geometry of these complexes can evolve from s.p. to t.b.p., depending on the nature of the ligands.

This behavior is clearly observed in the series of five SNS/S compounds [TcO{SN(etNEt$_2$)S}(HSPhBr)] [76a], [TcO{SN(etNEt$_2$)S}(STol)] [76b] (Fig. 16), [TcO{SN(etNEt$_2$)S}(Sbz)] [76c], [TcO{SN(etNEt$_2$)S}(SPhOMe)] [76d] (Fig. 16), [TcO(SN(etmorph)S)(Sbz)] [77] (SN(etmorph)S = *N*-ethylmorpholine bis(2-mercapto, 2-dimethylethyl)aminate $(2-)$) and in the SNS/Cl precursor [TcOCl(SN(etSEt)S)] [75] (Table 3, ii).

The τ values reported in Table 3 indicate that only complex 76d crystallizes in an s.p. arrangement ($\tau = 0.05$). On the other hand, complex [77] shows a significantly distorted s.p. geometry ($\tau = 0.42$), whereas the other species assume a distorted t.b.p. configuration ($0.61 < \tau < 0.68$). In t.b.p. complexes, the basal plane is realized by the thiolate atoms of the tridentate ligand and by the oxo group. The apical positions are occupied by the central nitrogen of the chelate and by the sulfur of the monothiol. Interestingly, the pendant fragment bonded to the N-donor of the tridentate ligand is usually syn-positioned with respect to the technetium oxo core. The systematic variation of the N-substitutents has also shown that the anti isomers rarely form, and always to a negligible extent. Furthermore, preparation of the syn isomers seems to be the key factor for achieving both high brain uptake and retention.

In the literature, two other compounds containing dianionic tridentate ligands in which the SNN donor atom set replaces the SNS one have also been described: [TcO{SNN(pyr)}(STol)] [78a] and [TcO{SNN(pip)}(Sbz)] [78b] (SNN(pip) = *N*-(2,2-dimethyl-2-mercaptoethyl)(2-piperidine) ethylaminate $(2-)$). Both derivatives have a monodentate thiol as co-ligand and the geometry around the metal is distorted s.p. ($\tau = 0.21$ and 0.25 respectively). In [78a] the pyrrolidine ring and the five-membered chelate rings adopt an envelope form.

The '3 + 1' approach also allows the insertion of a biofragment. Conjugation is generally expected to take place at the monodentate thiol, with the tridentate ligand devoted to complex stabilization. However, the strategy can be reversed, with the biological molecule bound to the tridentate donor as in [TcOCl(*Z*-Ala-dtc)] [40b] (Fig. 17), which contains a simple N-protected amino acid.

3.1.3. Other mono-oxo complexes

The ten complexes gathered in this section are reported in Table 3; so far, none of these molecules has a radiopharmaceutical application. All of them show octahedral coordination except for compound $[TcO(biguan)^2]^+$ [29b], which exhibits an s.p. geometry (Table 3, iii). Unlike in Sections 3.1.1 and 3.1.2, there are halogen atoms in nearly all structures. The coordination sphere usually includes a couple of bidentate ligands, except for $[TcOCl_3(malt)]^-$ [79], $[TcOCl_2(hdto)]$ [80a] and [TcO(HAF)(PAC)] [85] (HAF = *S*-methyl-*o*-*N*-(2-hydroxyphenylethylidene)dithiocarbazate (2 −); PAC = *S*-methyl-*o*-*N*-(isopropylidene) dithiocarbazate (1 −)), showing only a bidentate, a tridentate or a combination of a bidentate plus a tridentate ligand respectively.

In octahedral complexes the displacement of the metal ion towards the apical oxygen varies between 0.13 Å in [80a] and 0.29 Å in $[TcOCl(PO)_2]$ [83]. The O=Tc–$L_{(trans)}$ angle markedly deviates from linearity, yet it is restricted to a narrow range (156.8°–164.5°). The donor atom of the $L_{(trans)}$ ligand is invariably an oxygen, thereby generating 'twisted'-type bis-bidentate complexes, in which one ligand bridges an equatorial and an apical position, and the other two equatorial ones.

3.2. Di-oxo- and μ-oxo complexes.

Five structurally characterized Tc(V) di-oxo complexes are reported in this section. Normally, cationic di-oxo compounds are octahedral species with trans-po-

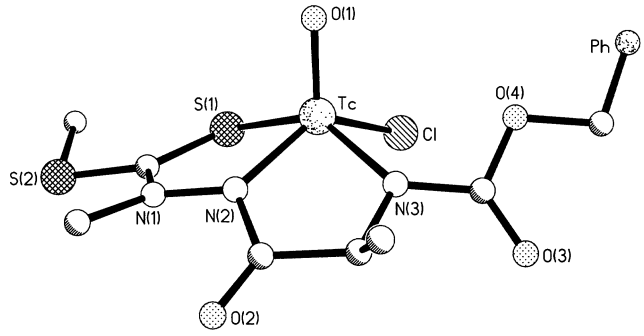

Fig. 17. [TcOCl(*Z*-Ala-dtc)] [40b]: a simple conjugation at the tridentate framework of biological significance.

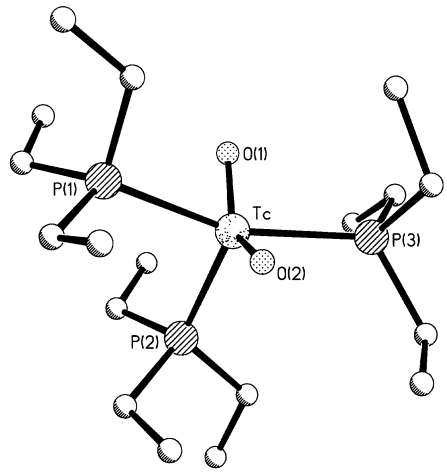

Fig. 18. A rare example of cis-di-oxo configuration: $[TcO_2(PEt_3)_3]^+$ [87a].

sitioned oxo groups, like $[TcO_2(tn)_2]I{\cdot}H_2O$ [86]. However, two of the compounds described in Table 4, $[TcO_2(PEt_3)_3]^+$ [87a] (Fig. 18) and $[TcO_2(PPr_3)_3]^+$ [87b], show an unusual and striking feature. They are five-coordinate and the geometry around the Tc atom is distorted t.b.p., with the two oxo ligands in the trigonal plane. Such a cis-di-oxo configuration affects the Tc–O bond distances, which range from 1.707(4) to 1.726(3) Å. These values are intermediate between those found in mono-oxo complexes [62–78] and trans-di-oxo compounds [86,87c,d]. Moreover, the mean apical Tc–P distance (2.517 Å) of cis-di-oxo derivatives is longer than those found in other neutral t.b.p. compounds. This feature indicates an attempt to overcome the steric interactions with the phosphine positioned in the basal plane.

Both $[TcO_2(PEt_3)_3]^+$ and $[TcO_2(PMe_3)_3]^+$ easily replace one phosphine with two pyridine ligands, again affording the classical trans-di-oxo octahedral arrangement, as shown by $[TcO_2(PMe_3)_2(py)_2]^+$ [87c] and $[TcO_2(PEt_3)_2(py)_2]^+$ [87d]. The equatorial plane is filled by phosphine and pyridine ligands, both cis-positioned.

Table 4 summarizes the main structural parameters of the six octahedral μ-oxo complexes. The linear $[Tc_2^{V}O_3]^{4+}$ core is found in $[(\mu\text{-O})\{TcOCl_2(dtdc)_2\}_2]$ [80b] and $[(\mu\text{-O})\{TcO(hbdp)_2\}_2]$ [88] (hbdp = *N*,*N*′-bis(2-hydroxybenzyl)-1,3-diamino-2(4-nitrobenzyl)propanate (2 −)), whereas the quasi-linear $[Tc_2^{III}O]^{4+}$ unit appears in $[(\mu\text{-O})\{TcCl(bpy)_2\}_2]^{2+}$ [89a], $[(\mu\text{-O})\{TcBr(bpy)_2\}_2]^{2+}$ [89b], $[(\mu\text{-O})\{TcCl(phen)_2\}_2]^{2+}$ [89c] and $[(\mu\text{-O})\{TcCl(tpy)(Me_2bpy)\}_2]^{4+}$ [90] (Fig. 19).

Studies on metal–metal interactions and electrochemical investigations aimed to explain the catalytic properties of dinuclear compounds containing a transition metal, such as Ru polypyridyl complexes, led to the synthesis of a series of similar μ-oxo Tc(III) complexes: $[(\mu\text{-O})\{TcCl(bpy)_2\}_2]^{2+}$ [89a], $[(\mu\text{-O})\{TcBr(bpy)_2\}_2]^{2+}$

Table 4
Some structural parameters for dioxo TcO_2^+ and octahedral μ-oxo complexes

Compound	Donor set	C.n.	O.n.	τ[a] (°)	Tc–$O_{(bridging)}$ (Å)	O_{oxo}–Tc–$L_{(trans)}$ (°)	Tc–O–Tc (°)	Δ[b] (Å)	O–Tc–O (°)	Ref.
$[TcO_2(tn)_2]^+$	N_4O_2	6	V					0.00	179.4(2)	[86]
$[TcO_2(PEt_3)_3]^+$	O_2P_3	5	V	0.83				0.00	142.4(2)	[87a]
$[TcO_2(PPr_3)_3]^+$	O_2P_3	5	V	0.79				0.00	141.5(2)	[87b]
$[TcO_2(PMe_3)_2(py)_2]^+$	$N_2O_2P_2$	6	V					0.02	175.1(5)	[87c]
$[TcO_2(PEt_3)_2(py)_2]^+$	$N_2O_2P_2$	6	V					0.03	173.1(4)	[87d]
(μ-O)$[TcOCl_2(dtdc)_2]_2$	$O_2S_2Cl_2$		V		1.898(3)	166.3(2)	174.9(1)	0.11		[80b]
(μ-O)$[TcO(hbdp)_2]_2$	N_2O_4		V		1.903(1)	163.4(4)	180	0.13		[88]
$\{(\mu\text{-O})[TcCl(bpy)_2]_2\}^{2+}$	N_4OCl		III		1.824(2)	167.4(3)	171.9(8)	0.16		[89a]
$\{(\mu\text{-O})[TcBr(bpy)_2]_2\}^{2+}$	N_4OBr		III		1.828(1)	167.8(1)	173.0(3)	0.17		[89b]
$\{(\mu\text{-O})[TcCl(phen)_2]_2\}^{2+}$	N_4OCl		III		1.819(3)	170.7(4)	171.6(9)	0.16		[89c]
$\{(\mu\text{-O})[Tc(tpy)\text{-}(Me_2bpy)]_2\}^{4+}$	N_5O		III		1.831(6)	174.1(2)	171.1(3)	0.18		[90]

[a] τ as in Table 1.
[b] Δ as in Table 3.

[89b] and $[(\mu\text{-O})\{TcCl(phen)_2\}_2]^{2+}$ [89c]. As expected, the compounds exhibit a high degree of isomorphism, being all slightly bent along the Tc–O–Tc axis and showing a staggered configuration of the halide ligands. A five-nitrogen-atoms donor set is present in [90], where the slight bending of Tc–O–Tc (171.1(3)°) allows an interaction between two of the three terpyridyl pyridine rings.

4. Technetium in low oxidation states

This crowded section hosts 56 structures with the metal in low oxidation states, usually from I to III. The compounds are divided into the following four subgroups: (i) complexes with a 'sulfur-rich' coordination sphere (Table 5), (ii) octahedral species containing π-acceptor ligands (Table 6), (iii) complexes showing the distinctive *fac*-$[Tc(CO)_3]^+$ fragment (Table 7) and (iv) genuine organometallic compounds.

4.1. Complexes with 'sulfur-rich' coordination sphere

This group gathers seven structures whose coordination sphere is largely supported by sulfur atoms; other donors include nitrogen and phosphorus atoms. Despite the small number of entries, this family shows a considerable diversity of o.n. (III, IV and V), c.n. (5, 6, 7 and 8) and geometry around the metal center (Table 5).

Consequently, the Tc–S distances are also heterogeneous, ranging from 2.224(2) Å in $[Tc\{N(CH_2CH_2S)_3\}(PPh_3)]$ [92] (Fig. 20) to 2.507(4) Å in $[Tc(S_3CPh)_2(S_2CPh)]$ [93] (Fig. 21).

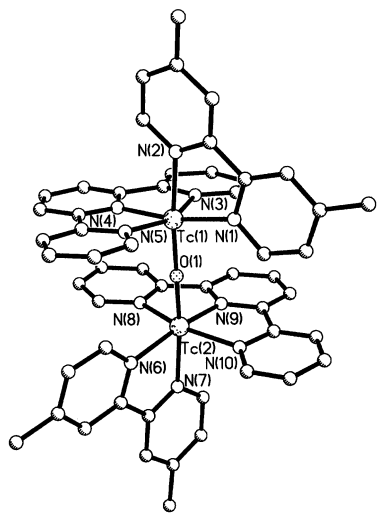

Fig. 19. The $[Tc–O–Tc]^{4+}$ moiety in $[(\mu\text{-O})\{TcCl(tpy)(Me_2bpy)\}_2]^{4+}$ [90].

Table 5
Complexes with 'sulfur-rich' coordination sphere

Compound	Donor set	O.n.	C.n.	Polyhedron	Tc–S (Å)	Ref.
$[Tc(SCH_2CH_2PPh_2)_2$-$(SCH_2CH_2P(O)Ph_2)]$	P_2S_3	III	5	tbp; 0.75[a]	2.232(5); 2.245(4); 2.256(3)	[91]
$[Tc\{N(CH_2CH_2S)_3\}(PPh_3)]$	NPS_3	III	5	tbp; 0.98[a]	2.224(2); 2.277(2); 2.228(2)	[92]
$[Tc(Smetetraz)_3(PPh_3)(NCCH_3)]$	NPS_3	III	5	tbp; 0.97[a]	2.233(2); 2.245(2); 2.248(7)	[21b]
$[Tc(S_3CPh)_2(S_2CPh)]$	S_6	III	6	tp; 9.6[b]	2.253(3); 2.228(3); 2.344(3); 2.353(3); 2.480(4); 2.507(4)	[93]
$[Tc(Etxan)_3(PMe_2Ph)]$	PS_6	III	7	pbp; 174.5[c]	2.436(1); 2.455(1); 2.456(1); 2.467(1); 2.479(1); 2.488(1)	[94a]
$[Tc_2(edt)_2(e{=}dt)_2]$	S_6	IV	6	tp; 6.0[b]	2.293(5); 2.297(6); 2.390(6); 2.392(5); 2.392(7); 2.394(4)	[95]
$[Tc(thiuram)_4]^+$	S_8	V	8	sa; 0.0[d]	2.463(2); 2.482(2); 2.491(2); 2.494(2)	[96]

[a] tbp; τ = trigonal bipyramid; $\tau = (\beta\text{-}\alpha)/60$, where α and β are the two largest angles around Tc.
[b] tp; ϕ (°) = trigonal prismatic; ϕ is the twist angle between the upper and lower triangular faces.
[c] pbp; η (°) = pentagonal bipyramid; η is the P–Tc–S_{trans} angle.
[d] sa; ε (°) = square antiprism; ε is the twist angle between the upper and lower square faces.

Table 6
Relevant structural data for octahedral complexes with mixed π-acceptor ligands.

Compound	Donor set	O.n.	Δ[a] (Å)	$X_{(apical)}$–Tc–$L_{(trans)}$ (Å)		Tc–P (Å)	Ref.
$[Tc(CN\text{-}t\text{-}bu)_5(PMe_2Ph)]^+$	C_5P	I	0.04	P–Tc–C	178.1(5)	2.403(6)	[97a]
$[Tc(CN\text{-}t\text{-}bu)_4(PMe_2Ph)_2]^+$	C_4P_2	I	0.00	P–Tc–P	180	2.392(3)	[97b]
trans-$[Tc(CN\text{-}t\text{-}bu)_2(dppe)_2]^+$	C_2P_4	I	0.00	C–Tc–C	180	2.421(2); 2.432(2)	[98]
$[Tc(=C=CHPh)Cl(dppe)_2]$	CP_4Cl	I	0.04	C–Tc–Cl	177.7(3)	2.397(2); 2.423(3)2.427(3); 2.434(2)	[99a]
$[Tc(\equiv CCH_2\text{-}t\text{-}bu)Cl(dppe)_2]^+$	CP_4Cl	I	0.13	C–Tc–Cl	175.9(3)	2.453(3); 2.487(3)2.491(3); 2.538(3)	[99b]
$[Tc(NCCH_3)_6]^{2+}$	N_6	II	0.00	N–Tc–N	180		[100]
$[Tc(bpy)_3]^{2+}$	N_6	II	0.00	N–Tc–N	180		[101a]
$[TcCl(tpy)\ (py)_2]$	N_5Cl	I	0.15	Cl–Tc–N	180.0(1)		[102a]
trans-$[TcCl_2(NCCH_3)_4]^+$	N_4Cl_2	III	0.00	Cl–Tc–Cl	180		[103a]
trans-$[TcCl_2(py)_4]$	N_4Cl_2	II	0.00	Cl–Tc–Cl	180		[102b]
trans-$[TcCl_2(py)_3(PPh_3)]^+$	N_3PCl_2	III	0.00	Cl–Tc–Cl	176.5(1)	2.472(2)	[102c]
$[TcCl_4(py)_2]^-$	N_2Cl_4	III	0.00	N–Tc–N	180		[104a]
$[TcBr_4(py)_2]^-$	N_2Br_4	III	0.00	N–Tc–N	180		[104b]
trans-$[TcCl_2(NCS)(PMe_2Ph)_3]$	NP_3Cl_2	III	0.04	Cl–Tc–Cl	177.2(1)	2.443(1); 2.478(1)2.482(1)	[105]
$[TcCl_3(NCCH_3)\{P(C_6H_4Me\text{-}3)_3\}_2]$	NP_2Cl_3	III	0.08	Cl–Tc–N	177.7(1)	2.492(1); 2.501(1)	[101b]
mer-$[Tc(O_2CCH_2CH_2PPh_2)_3]$	O_3P_3	III	0.03	O–Tc–O	179.0(2)	2.393(2); 2.478(2); 2.479(2)	[106]
trans-$[Tc(dppe)_2(OH_2)_2]^+$	O_2P_4	I	0.03	O–Tc–O	175.7(2)	2.493(2); 2.498(2); 2.502(2); 2.505(2)	[107]
$[Tc(dmdc)(depe)_2]^+$	P_4S_2	II	0.02	P–Tc–P	172.8(1)	2.364(2); 2.397(2); 2.420(2); 2.442(2)	[108]
cis-$[Tc(SPh)_2(dmpe)_2]^+$	P_4S_2	III	0.20	S–Tc–P	170.5(2)	2.409(5); 2.426(5); 2.467(6); 2.510(5)	[109]
$[Tc(SCP)_2(dmpe)_2]^+$	P_4S_2	III	0.00	S–Tc–S	180	2.431(2); 2.442(2)	[110]
$[Tc(PMe_2Ph)_2(dmpe)Cl_2]$	P_4Cl_2	II	0.01	Cl–Tc–Cl	179.4(1)	2.398(4); 2.400(4); 2.431(5); 2.434(4)	[111]
trans-$[TcCl_2(Et_2dtp)(PMe_2Ph)_2]$	$P_2S_2Cl_2$	III	0.01	Cl–Tc–Cl	174.1(1)	2.424(1); 2.440(1)	[112]
trans-$[TcCl_2(Me_2dtp)(PMe_2Ph)_2]$	$P_2S_2Cl_2$	III	0.00	Cl–Tc–Cl	173.0(1)	2.416(1)	[94b]
trans-$[TcCl_4(PMe_3)_2]$	P_2Cl_4	IV	0.00	P–Tc–P	180	2.524(2)	[113a]

[a] Δ is the displacement of Tc from the basal plane towards the donor.

Table 7
Complexes with a *fac*-$[Tc(CO)_3]^+$ fragment

Compound	Donor set	Δ[a] (Å)	OC–Tc–$L_{(trans)}$ (°)	Θ[b] (°)	Ref.
$[Tc(CO)_3(CN\text{-}t\text{-}bu)_3]^+$	C_6	0.05	173.7(1)	3.7	[118a]
$[Tc(CO)_3Cl(CN\text{-}t\text{-}bu)_2]$	C_5Cl	0.04	177.9(2)	2.8	[119]
$[Tc(CO)_3Br(en)]$	C_3N_2Br	–[c]	179.1(3)	–[c]	[120a]
$[Tc(CO)_3Cl(N \cap Narylpip)]$	C_3N_2Cl	0.08	172.5(1)	3.9	[121]
$[Tc(CO)_3\{(SPPh_2)_2N\}(NCCH_3)]$	C_3NS_2	0.05	173.9(3)	2.7	[122]
$[Tc(CO)_3\{HB(C_3H_3N_2)_3\}]$	C_3N_3	0.06	176.0(1)	0.0	[123a]
$[Tc(CO)_3\{HB(3,5\text{-}Me_2C_3HN_2)_3\}]$	C_3N_3	0.01	175.3(6)	3.1	[123b]
$[Tc(CO)_3(9\text{-ane-}S_3)]^+$	C_3S_3	0.06	179.0(2)	3.2	[124a]
$[Tc_2(CO)_6(tosylate)(18\text{-ane-}S_6)]$	C_3S_2O	0.04c	177.4(2)	3.1	[124b]
$[Tc_2(CO)_6(20\text{-ane-}S_6\text{-}OH)]^{2+}$	C_3S_3	0.05	175.2(4)	1.0	[124c]
$[Tc_2(CO)_6(\mu\text{-}SCH_2CH_2OH)_3]^-$	C_3S_3	0.12	173.7(1)	1.1	[118b]
$[Tc_2(CO)_6(\mu\text{-}Cl\}_3]^-$	C_3Cl_3	0.05	174.2(3)	1.3	[125]
$[Tc(CO)_3(\mu_3\text{-}Cl)]_4$	C_3Cl_3	–[c]	175.8(1)	–[c]	[120b]
$[Tc_3(CO)_{12}(\mu_2\text{-}H)_3]$	C_4H_2	0.11[d] mean	167(2) mean	12.2 mean	[126]

[a] Δ is the displacement of Tc from the basal plane towards the apical CO ligand.
[b] Θ is the dihedral angle between the tricarbonyl triangular C_3 face and the opposite one.
[c] Unavailable data.
[d] Far from the apical CO group.

If the metal is five-coordinate, the complexes assume a t.b.p. arrangement by placing three thiolate groups at the trigonal base and π-acceptor P and N atoms at the apices. The Tc–S distances vary in a narrow range, from 2.224 (2) Å in [92] to 2.248(7) Å in $[Tc(Smetetraz)_3(PPh_3)(NCCH_3)]$ [21b]. Complex [92] shows the rather unusual '4 + 1' mixed-ligand sphere, but still retains the t.b.p. array. When the c.n. becomes greater, the Tc–S distances lengthen up to 2.483(2) Å in the eight-coordinate complex $[Tc(thiuram)_4]^+$ [96] (Fig. 22). The latter is the unique complex in the review, showing such a large coordination number.

The pentagonal bipyramidal complex $[Tc(Etxan)_3(PMe_2Ph)]$ [94a] (Fig. 23) is one of the few compounds showing c.n. = 7. In this complex the Tc atom deviates by 0.10 Å from the pentagonal basal plane towards the apical P donor and the equatorial S–Tc–S angles vary between 68.60 and 76.3° compared with the ideal value of 72°.

Two more complexes deserve comment. The dimeric complex $[Tc_2(edt)_2(e{=}dt)_2]$ [95] is an original example of o.n. IV and the first reported species containing two terminal dithiolene and two bridging dithiolato ligands. The two dithiolato ligands provide four μ_2-sulfur atoms to yield a quadruply bridged Tc(IV) dimer, in which

the mean Tc–S distance is 2.392(5) Å. Another example of a coordination sphere totally filled by sulfur atoms is the six-coordinate $[Tc(S_3CPh)_2(S_2CPh)]$ [93] (Fig. 21), which combines two perthiobenzoate and one dithiobenzoate ligands around the Tc(III) ion. In the distorted trigonal prism environment three types of metal-sulfur interaction can be identified, according to the different nature of coordinated sulfur, i.e. covalent perthio-S (2.226(3) Å), co-ordinative perthio-S (2.348(3) Å) and dithiobenzoato-S (2.507(4) Å).

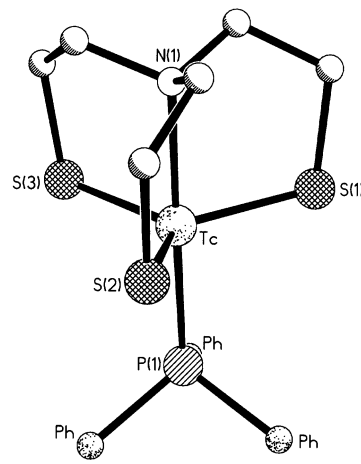

Fig. 20. Five-coordinate $[Tc\{N(CH_2CH_2S)_3\}(PPh_3)]$ [92] exhibiting t.b.p. geometry.

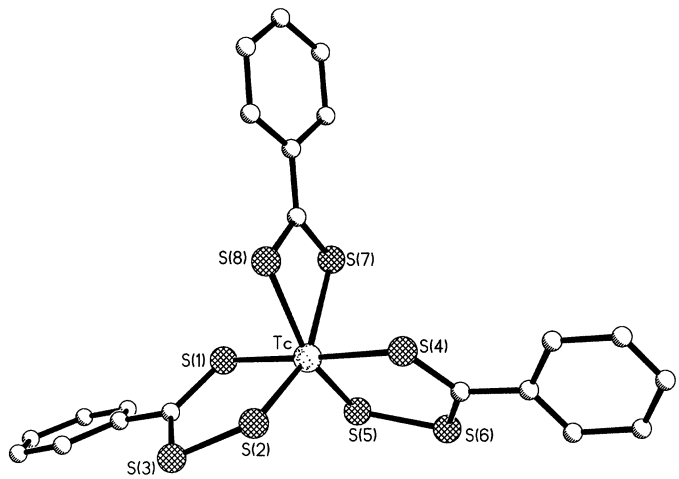

Fig. 21. Six-coordinate $[Tc(S_3CPh)_2(S_2CPh)]$ [93] with trigonal prismatic arrangement.

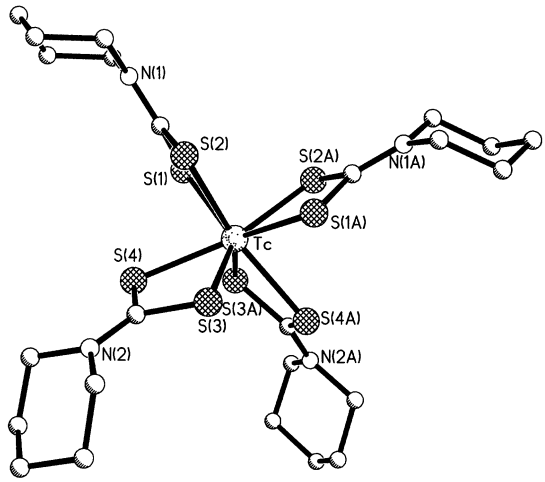

Fig. 22. A unique example of an eight-coordinate Tc(V) complex: $[Tc(thiuram)_4]^+$ [96].

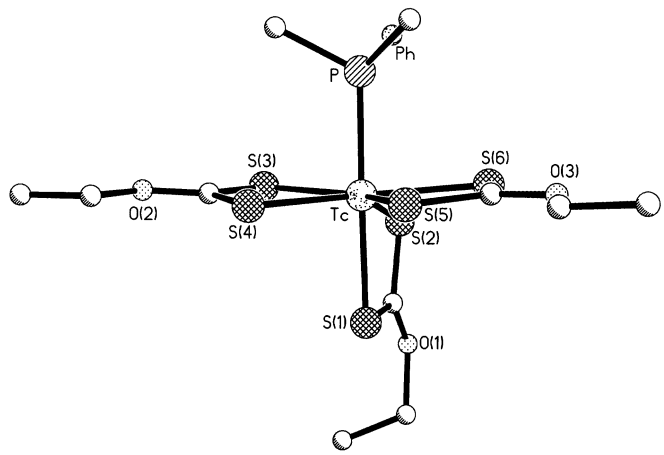

Fig. 23. Seven-coordinate $[Tc(Etxan)_3(PMe_2Ph)]$ [94a] showing a pentagonal bipyramidal geometry.

4.2. Complexes with mixed π-acceptor ligands

This family contains 28 structures (Table 6), 24 of which are octahedral complexes. The technetium ion exhibits several o.ns: III (14 structures), I (eight structures), II (five structures) and IV (one structure). About half these compounds are neutral, 13 complexes are cationic, three of which are dicationic entities, and two complexes are monoanionic compounds. The most represented donor atoms are phosphorus (34.7%), nitrogen (23.6%) and chlorine (19.4%). On no occasion are oxygen and nitrogen simultaneously present in the donor set.

The Tc–P distances vary between 2.364(2) Å in $[Tc(dmdc)(depe)_2]^+$ [108] and 2.538(3) Å in $[Tc(\equiv CCH_2\text{-}t\text{-}bu)Cl(dppe)_2]^+$ [99b]. In the latter, all the Tc–P distances appear to be elongated. The four phosphorus atoms move away from the metal, which is involved in a very short bond with the carbyne atom (1.724(7) Å). Also, the Tc–Cl bond trans to the carbyne is longer than usual (2.523(3) Å). A similar arrangement is found in $[Tc(=C=CHPh)Cl(dppe)_2]$ [99a], where the Tc=C (carbene) distance is 1.861(9) Å.

The Tc–P distances become longer when the metal increases its o.n. from III to IV. Thus, the Tc–P distance is 2.416(1) Å in *trans*-$[TcCl_2(Me_2dtp)(PMe_2Ph)_2]$ [94b] and 2.524(2) Å in *trans*-$[TcCl_4(PMe_3)_2]$ [113a]. The Tc–Cl distances do not deviate appreciably from 2.35 Å, unless the trans-effect operates. By contrast, there is considerable variety in the Tc–N distances, depending on the metal o.n. and on the chemical nature of the nitrogen. The shortest Tc–N distance is 1.915(7) Å in $[TcCl(tpy)(py)_2]$ [102a], and the longest is 2.218(5) Å in *trans*-$[TcCl_2(py)_3(PPh_3)]^+$ [102c]. The first value refers to a Tc(I) bound to the internal nitrogen of the terpyridine ligand, the last one to a Tc(III) bound to the nitrogen of the pyridine trans to the bulky PPh_3 group.

Only a few complexes do not show c.n. = 6. Two of these structures, namely $[Tc(NCS)\{(CDOH)_2(CDO)\}BMe]$ [114] ($(CDOH)_2(CDO)Bme$ = [1,2-cyclohexanedione dioximate][1,2-cyclohexanedione dioximate]methylborate $(3-)$) and $[TcCl(dmg)_3BTol]$ [115], are seven-coordinate boronic acid adducts of technetium dioxime complexes (BATOs) [11]. This class of compounds has yielded a prototype molecule for myocardial imaging [116]. The coordination sphere around the metal is monocapped trigonal prismatic. The capped position is held by the thiocyanate [114] or by the chloride [115] ligand and the capped face is realized by the four nitrogen atoms of two bidentate ligands.

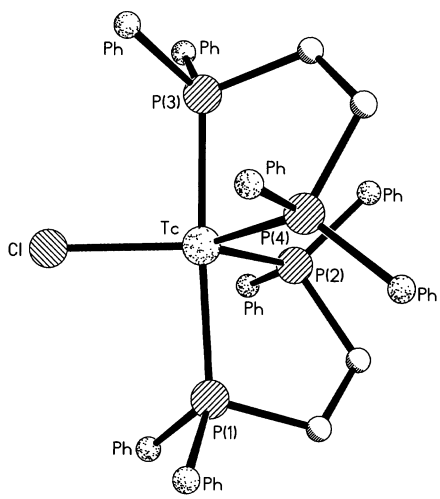

Fig. 24. The electron-deficient compound $[TcCl(dppe)_2]$ [117a].

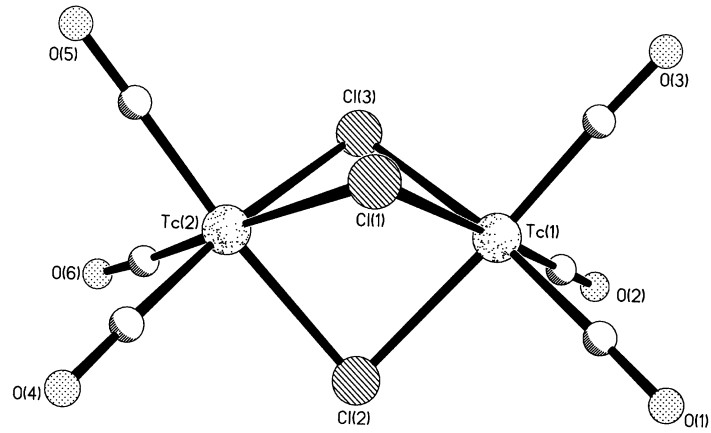

Fig. 25. The anionic dimer $[Tc_2(CO)_6(\mu\text{-}Cl)_3]^-$ [125], an intermediate species in the reduction of pertechnetate to the *fac*-$[Tc(CO)_3]^+$ synthon.

The complex $[TcCl(dppe)_2]$ [117a] (Fig. 24) is the sole molecule that shows c. n. = 5. The geometry about technetium is distorted trigonal bipyramidal ($\tau = 0.63$). The $P_{(apical)}$–Tc–$P_{(apical)}$ angle is 175.2(1)°, the Tc–$P_{(apical)}$ mean distance is 2. 367 (2) Å and the Tc–$P_{(basal)}$ distance is 2.240(2) Å.

If the intense green benzene solution of this complex is treated with hydrogen, the yellow compound *trans*-$[TcCl(H_2)(dppe)_2]$ [117b] is obtained, as the first η^2-dihydrogen complex of technetium. Its structure is octahedral, with the technetium atom lying on a crystallographic inversion center.

4.3. Complexes containing the fac-[Tc(CO)$_3$]$^+$ fragment

At the beginning of the 1990s the organometallic moiety *fac*-$[Tc(CO)_3]^+$ was found to be an extremely versatile synthon able to generate an unexpected rich aqueous chemistry through the *fac*-$[Tc(CO)_3(OH_2)_3]^+$ aqua-ion [16]. In this fragment, the kinetic inertness of the small *fac*-$[Tc(CO)_3]^+$ moiety is accomplished with the substitution lability of the solvent ligands, making feasible the synthesis of several mixed-ligand species. Hence, the tricarbonyl metal fragment is emerging among the most investigated moieties for radiopharmaceutical development.

In this connection, 14 complexes containing the *fac*-$[Tc(CO)_3]^+$ moiety have been structurally characterized (Table 7).

The metal always shows o.n. I and c.n. = 6. The complexes are mostly neutral; three compounds are cationic $[Tc(CO)_3(CN\text{-}t\text{-}bu)_3]^+$ [118a], $[Tc(CO)_3(9\text{-ane-}S_3)]^+$ [124a] and $[Tc_2(CO)_6(20\text{-ane-}S_6\text{-OH})]^{2+}$ [124c], and only two are anionic $[Tc_2(CO)_6(\mu\text{-}Cl)_3]^-$ [125] (Fig. 25) and $[Tc_2(CO)_6(\mu\text{-}SCH_2CH_2OH)_3]^-$ [118b].

Carbon atoms, coming from either π-acceptor carbonyl or isonitrile groups, represent the most recurrent donors (57.1%), in agreement with the electron-rich d^6 configuration exhibited by the Tc(I) ion. Other donors include additional π-accep-

tors such as thioether sulfur (15.5%), aromatic nitrogen (13.1%) and halogens (10.7%). In these complexes the tricarbonyl metal fragment is often supported by additional monodentate groups that fill the other face of the octahedron. Examples include the mixed carbonyl/isonitrile complexes $[Tc(CO)_3(CN\text{-}t\text{-}bu)_3]^+$ [118a] and $[Tc(CO)_3Cl(CN\text{-}t\text{-}bu)_2]^-$ [119] and some polynuclear species, such as $[Tc(CO)_3(\mu_3\text{-}Cl)]_4$ [120], $[Tc_2(CO)_6(\mu\text{-}Cl)_3]^-$ [125] and the μ-hydrido $[Tc_3(CO)_{12}(\mu_2\text{-}H)_3]$ (Fig. 26).

The distortion from the ideal octahedral geometry is measured by the parameter Θ (Table 7), i.e. the dihedral angle between the triangular face formed by the carbon atoms of the $[Tc(CO)_3]^+$ moiety and that arising from the opposite donors. As $\Theta = 0$ for the ideal octahedron, data in Table 7 indicate that in these complexes there is no significant distortion, with the exception of some polynuclear species like [126] and [118b]. In the latter the thiolate ligands afford a 'triple μ-thiolato-bridged dimer'.

The derivatives where a tridentate donor (or a combination of a bidentate plus a monodentate ligand) coordinate the face of the octahedron opposite to the face formed by the tri-carbonyl carbon atoms look much more interesting for clinical applications. In this view, the complex $[^{99m}Tc(CO)_3Cl(N \cap Narylpip)]$ [121] ($N \cap Narylpip = 4\text{-}(3\text{-}imino(2\text{-}pyridine)propyl)\text{-}1\text{-}(2\text{-}methoxyphenyl)\text{-}piperazine$) (Fig. 27) represents the first example of a bio-organometallic molecule, in which the pharmacophore retains its affinity in vitro for $5\text{-}HT_{1A}$ receptors when coordinated to the metal.

Three more complexes carry simple unsubstituted bidentate ligands: $[Tc(CO)_3Br(en)]$ [120a], $[Tc(CO)_3\{(SPPh_2)_2N\}(NCCH_3)]$ [122] and the dimer $[Tc_2(CO)_6(tosylate)(18\text{-}ane\text{-}S_6)]$ [124b]. Finally, tris-pyrazolyltorate and crown thioether ligands provide suitable tridentate frameworks to stabilize the tricarbonyl metal fragment, as shown by $[HB(C_3H_3N_2)_3Tc(CO)_3]$ [123a], HB(3,5-

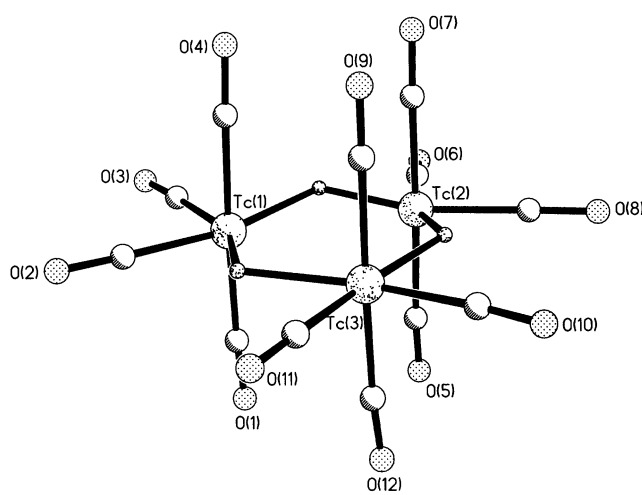

Fig. 26. The six-membered Tc_3H_3 ring in the unusual μ-hydrido derivative $[Tc_3(CO)_{12}H_3]$ [126].

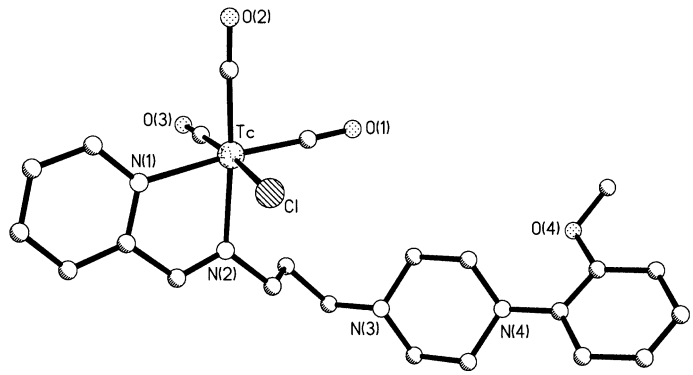

Fig. 27. The first example of a bio-organometallic molecule: $[Tc(CO)_3Cl(N \cap Narylpip)]$ [121].

$Me_2C_3HN_2)_3Tc(CO)_3]$ [123b], $[Tc(CO)_3(9\text{-ane-}S_3)]^+$ [124a] and $[Tc_2(CO)_6(20\text{-ane-}S_6OH)]^{2+}$ [124c].

4.4. Organometallic complexes

Despite the widespread use of $[Tc(CNR)_6]^+$ [11] as a myocardial agent and the potential application of the tricarbonyl derivatives just described, the development of organometallic technetium chemistry is rather limited. This section deals with seven neutral compounds, all containing the metal with o.n. = I, stabilized by ancillary polyhapto-ligands, namely cyclopentadienide or polypyrazolylborate. Straightforward exchange reactions of the Tc(I) carbonyl compound $[TcBr(CO)_5]$ with the appropriate alkali salts give the already-mentioned $[HB(C_3H_3N_2)_3Tc(CO)_3]$ [123a], $HB(3,5\text{-}Me_2C_3HN_2)_3Tc(CO)_3]$ [123b] and the atypical complex $[Tc(CO)_3(\eta^5\text{-}Me_4C_4N)]$ [127]. In the latter, a tetramethylpyrrolyl ring is η^5-coordinated to the $[Tc(CO)_3]^+$ fragment, thus producing a heterocyclic 'half-sandwich' structure with the three carbonyl carbon atoms lying in a plane parallel to the η^5-coordinate ring. Compounds [123a] and [123b] proved, in turn, to be useful precursors for the photochemical synthesis of $[\{[HB(3,5\text{-}Me_2C_3HN_2)_3]Tc(CO)_2\}_2(\mu\text{-}N_2)]$ [128] (Fig. 28), an unprecedented symmetrical N_2-bridged binuclear compound, where Tc shows a quasi-octahedral coordination. In this complex, the Tc–N–N, angle is 174(1)° and the N–N distance is about 0.06 Å longer than the distance found in dinitrogen.

Reaction of irradiated [123b] with trimethylphosphite and diphenylmethylphosphine gives $HB(3,5\text{-}Me_2C_3HN_2)Tc(CO)_2(P(OMe)_3)]$ [129a] and $[HB(H_3C_3N_2)_3\text{-}Tc(CO)(PPh_2Me)_2]$ [129b] respectively.

Three more organometallic compounds have been structurally characterized: $[\eta^5\text{-}CpTc(CO)_2PPh_3]$ [129c], $[\eta^5\text{-}Cp^{Me}Tc(CO)_2PPh_3]$ [129d] and $[\eta^5\text{-}Cp^{Me}(CO)_2Tc{=}C(OEt)Ph]$ [130]. In all these compounds, the $Tc\text{–}Cp_{centroid}$ distances are slightly longer (1.966(1) Å) than found in the precursors $[CpTc(CO)_3]$ and $[Cp^{Me}Tc(CO)_3]$ (1.944 (6) Å) [127].

As expected, the Tc–P distances in [129c] and [129d], 2.341(1) Å and 2.340(1) Å respectively, are longer than those found in [{$HB(3,5\text{-}Me_2C_3HN_2)_3$}$Tc(CO)_2$-$P(OMe)_3$] [129a] (2.299(5) and 2.327(5) Å), according to the different π-character and bulkiness of the P-substituents.

If the Cp^{Me} centroid is considered as one of the vertices, the compound [μ^5-$CpMe(CO)_2Tc{=}C(OEt)Ph$] [130] shows a pseudo-tetrahedral geometry. The C–Tc–Cp^{Me} centroid angles range from 117.5(4) to 130.0(4)°, and the sp^2-hybridization of the carbene carbon with respect to the sp one in [$Tc(=C{=}CHPh)Cl(dppe)_2$] [99a] leads to a longer Tc=C distance (1.977(1) versus 1.861(9) Å). Interestingly, the carbene group is oriented nearly perpendicular to the Cp^{Me} ligand.

5. Dinuclear complexes

Tc–Tc multiply bonded complexes have been investigated exclusively by Cotton and coworkers (Table 8), the only exception being $[Tc_2Cl_4(dppm)_2]$ [131]. This complex is a close analog of the β-form of Cotton's $[Tc_2Cl_4(dppe)_2]$ [132b], the first reported example of a Tc–Tc multiply bonded species containing bridging phosphine ligands. In [131] the coordination around each Tc is essentially t.b.p. ($\tau = 0.87$), whereas in [132b] the geometry is intermediate between t.b.p. and s.p. ($\tau = 0.48$). In the α-form of $[Tc_2Cl_4(dppe)_2]$ [132a] each dppe chelates only one metal atom, whereas in the β-form it bridges both Tc centers.

The c.n. around Tc is usually five, except for the two metal centers in $[Tc_2(NCCH_3)_8(CF_3SO_3)_2]^{2+}\cdot CH_3CN$ [103b] (Fig. 29) and one metal center in $[Tc_2Cl_4(DPhF)_4]\cdot C_7H_8$ [135a] which exhibit octahedral environments.

In s.p. complexes each Tc atom lies off the equatorial plane towards the other Tc center. Such a displacement varies between 0.16 Å in $[Tc_2Cl_4(DPhF)_4]\cdot C_7H_8$ [135a]

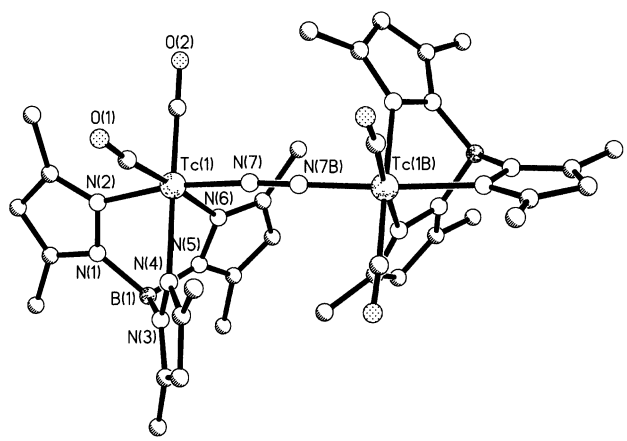

Fig. 28. An unprecedented symmetrical N_2-bridged binuclear compound: [{[$HB(3,5\text{-}Me_2C_3HN_2)_3$]$Tc(CO)_2$}$_2$($\mu$-$N_2$)] [128].

Table 8
X-ray structures of Tc–Tc multiply bonded complexes solved by Cotton's group

Compound	Donor set	Tc–Tc (Å)	Ref.
$[Tc_2Cl_4\{dppe)_2]$ (α-form)	$TcCl_2P_2$	2.15(1)	[132a]
$[Tc_2Cl_4(dppe)_2]$ (β-form)	$TcCl_2P_2$	2.117(1)	[132b]
$[Tc_3Cl_4(PEt_3\}_4]$	$TcCl_2P_2$	2.133(3)	[133a]
$[Tc_2Cl_4(PMe_2Ph)_4]$	$TcCl_2P_2$	2.127(1)	[133b]
$[Tc_2Cl_4(PMe_2Ph)_4]^+$ (orthorhombic)	$TcCl_2P_2$	2.109(1)	[134a]
$[Tc_2Cl_4(PMe_2Ph)_4]^+$ (monoclinic)	$TcCl_2P_2$	2.106(1)	[134b]
$[Tc_2Cl_4(PMe_2Ph)_4]^+ \cdot 1/2THF$	$TcCl_2P_2$	2.107(1)	[134c]
$[Tc_2Cl_4(PMePh_2)_4] \cdot C_6H_6$	$TcCl_2P_2$	2.138(1)	[133c]
$[Tc_2Cl_5(PMe_2Ph)_3]$	$TcCl_2P_2$ $TcCl_3P$	2.109(1)	[134d]
$[Tc_2Cl(DPhF)_4] \cdot C_7H_8$	$TcClN_4$ TcN_4	2.119(2)	[135a]
$[Tc_2Cl_2(DTolF)_3]$	$TcClN_3$	2.094(1)	[135b]
$[Tc_2(NCCH_3)_8(CF_3SO_3)_2]^{2+} \cdot CH_3CN$	$TcON_4$	2.122(1)	[103b]

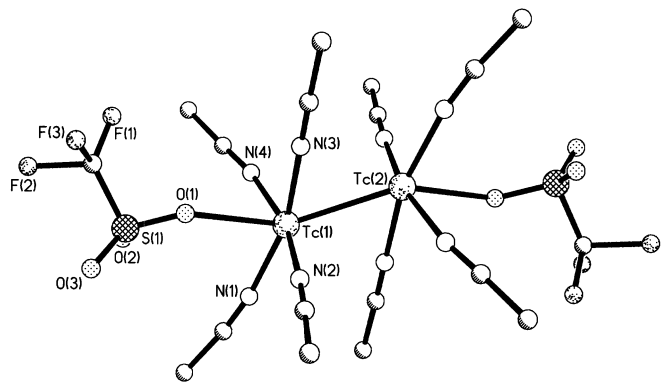

Fig. 29. The low-valent labile precursor $[Tc_2(NCCH_3)_8(CF_3SO_3)_2]^{2+}$ [103b].

and 0.73 Å in $[Tc_2Cl_4(PMePh_2)_4] \cdot C_6H_6$ [133c], and increases up to 0.93 Å in [103b], where the Tc atoms have an octahedral environment. Most of the complexes of the section display the two equivalent P_2Cl_2Tc donor set. The two compounds $[Tc_2Cl_5(PMePh)_3]$ [134d] and $[Tc_2Cl_4(DPhF)_4] \cdot C_6H_6$ [135a] show a different environment around each metal: PCl_3Tc/P_2Cl_2Tc and $NdClTc/N_4Tc$ respectively. The Tc–Tc distance changes very little (Table 8) and falls in the narrow range between 2.094 (1) Å in $[Tc_2Cl_2(DTolF)_3]$ [135b] and 2.138(1) Å in $[Tc_2Cl_4(PMePh_2)4] \cdot C_6H_6$ [133c]. Such a distance does not seem to be related with the complex charge.

A total of 16 dinuclear complexes have been classified in previous sections on the basis of other relevant features. Here we describe only the characteristic complex $[Tc_2(\mu,\eta^1,\eta^2\text{-}NCCH_3)(NCCH_3)_{10}]^{3+}$ [136] (Fig. 30). In this compound, the two Tc centers are bridged by an acetonitrile molecule that is bonded to one Tc atom via the lone pair on the nitrogen and to the second Tc atom in an η^1 fashion using the filled π-orbitals of the C≡N group. The Tc–Tc distance of 4.047(1) Å precludes any metal–metal bond interaction between the technetium centers.

6. Miscellaneous

The solid-state structures of pertechnetate compounds [120,137,138] are not discussed in this review, as they show no relevant data. The same applies to the structures containing the $[TcCl_6]^{2-}$ [113,120,139] and $[Tc_6I_{14}]^{3-}$ [120,140] anions. Other structures neither described nor discussed are the nitrido and di-oxo species solely with halide donors, i.e. $[TcNCl_4]^-$ [33,141–143], $[TcO_2F_3]$ [144] and $[TcO_2F_4]^-$ [145], together with the $[Tc_6X_8]$ cluster [146] and the $[TcS_2]$ dichalcogenides [147]. Finally, the structures of $[Tc(CO)_3I]_4$, $[Tc(CO)_5I]$, $[Tc(CO)_4I]_2$ and $[Tc_4(CO)_{12}F(OH)_3]$ have been elucidated by Grigorev et al. [148].

During the preparation of this review some more structures have appeared in the literature. They are briefly outlined below and assigned to the pertinent section. [TcO(SSS)Cl] [149] and [TcO(SN(pip)S)(SC_6H_4-*p*-Me)] [150] are two additional examples of the '3 + 1' approach (Section 3.1.2) presenting significant modification of the tridentate backbone. In the former complex a thioether sulfur has been inserted as central donor; in the latter, the tridentate framework carries the biological fragment.

The structure of a ^{99m}Tc-sestamibi analog, $[Tc(CNCH_2COOMe)_6]^+$ [151], has been elucidated as an octahedral Tc(I) species (Section 4.2).

Looking for novel oxo-free coordination spheres, a series of 'sulfur-rich' t.b.p. Tc(III) mixed-ligand complexes (Section 4.1), referred to as '3 + 1 + 1' or '4 + 1', has been proposed and sketched in Scheme 2 [152,153]. '3 + 1 + 1' species possess a combination of a tridentate dithiolato ligand, a monothiolato and a tertiary phosphine arranged to give the sulfur atoms at the trigonal base. The same basal coordination is shown in the '4 + 1' system, where a nitrile acts as monodentate co-ligand.

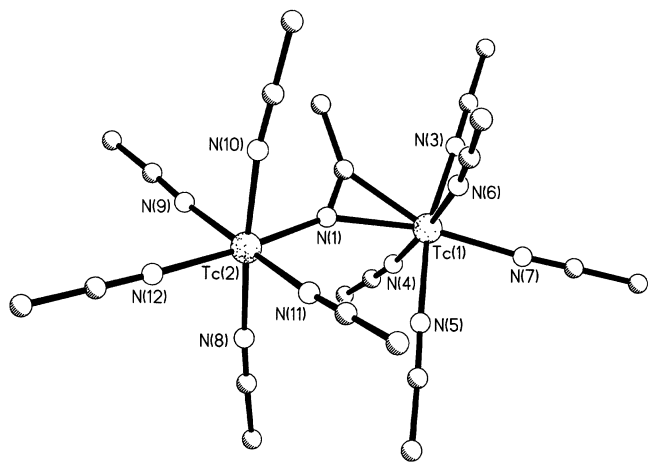

Fig. 30. The strange μ,η^1,η^2-ligating mode of acetonitrile among others η^1-acting in $[Tc_2(\mu,\eta^1,\eta^2\text{-}NCCH_3)(NCCH_3)_{10}]^{3+}$ [136].

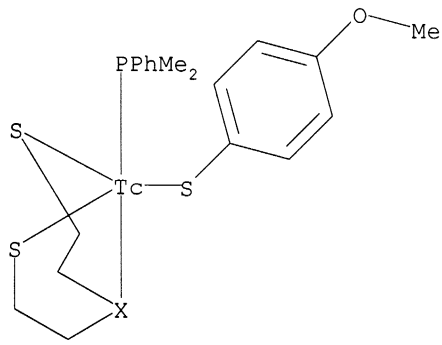

	X	Ref.
1.	O	[153a]
2.	NMe	[153b]
3.	S	[153c]

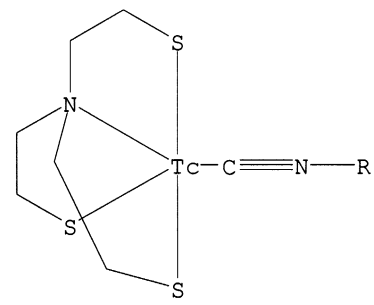

	R	Ref.
4.	benzyl	[154a]
5.	cyclohexyl	[154b]
6.	$(CH_2)_3N(Me)(CH_2)_3OPh$	[154c]
7.	$CH_2C(O)OEt$	[154d]

Scheme 2.

Finally, another $[TcNCl_4]^-$ anion [154] (this section) deserves mention for the unusually high-valent $[Au(Et_2dtc)_2]$ countercation, which places one dithiocarbamate sulfur trans to the nitrido group.

7. Conclusions

The present review collects the structural data of technetium complexes published in the years from 1993 to 1999. In this period 196 new single-crystal X-ray structure determinations have been performed, which accumulate with the 316 analyses described in the previous literature coverage [2–4].

Fig. 31 summarizes technetium structures as a function of the o.n. and c.n. The statistics include all X-ray determinations since 1965, with the exception of polynuclear, mixed-valent, organometallic and polycharged complexes.

Complexes showing odd o.n. V, III and I, which correspond to spin-paired d^2, d^4 and d^6 electronic configurations, are by far the most investigated, covering 49%, 22%, and 11% of the entries respectively. As expected, five-coordinate (32%) and six-coordinate (62%) species are largely favored, as well as neutral complexes (60%), compared with cationic (17%) and anionic (23%) compounds.

Fig. 32 depicts the ligating atoms as a function of the o.n. in the complexes examined within this structural survey. It appears that N, P, S and X (halides) represent the most recurrent donors, largely irrespective of the o.n. Conversely, O and C strongly prefer o.n. V and I respectively.

A detailed inspection of the coordination sphere of Tc(V) complexes bearing characteristic cores reveals that di-oxo and imido species are stabilized by a combination of N,P and P,X donors respectively (Fig. 33).

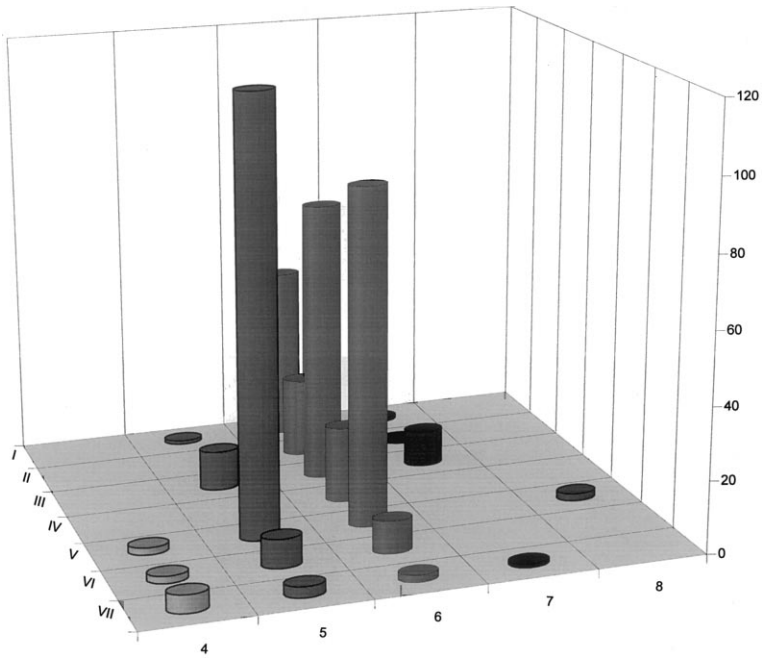

Fig. 31. Distribution of c.n. versus o.n. in Tc complexes.

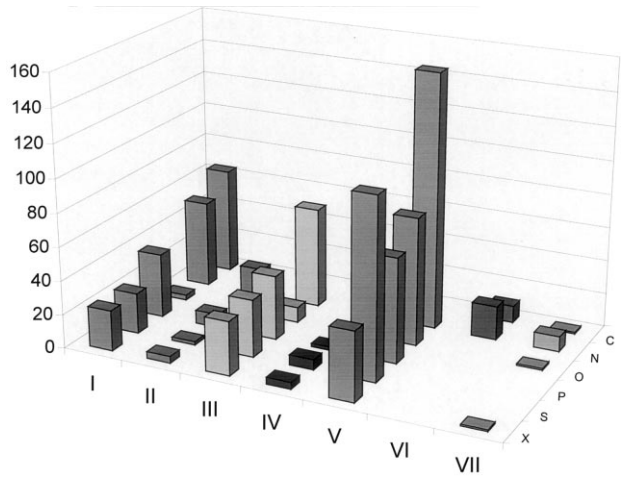

Fig. 32. Distribution of coordinating atoms versus o.n. in Tc complexes.

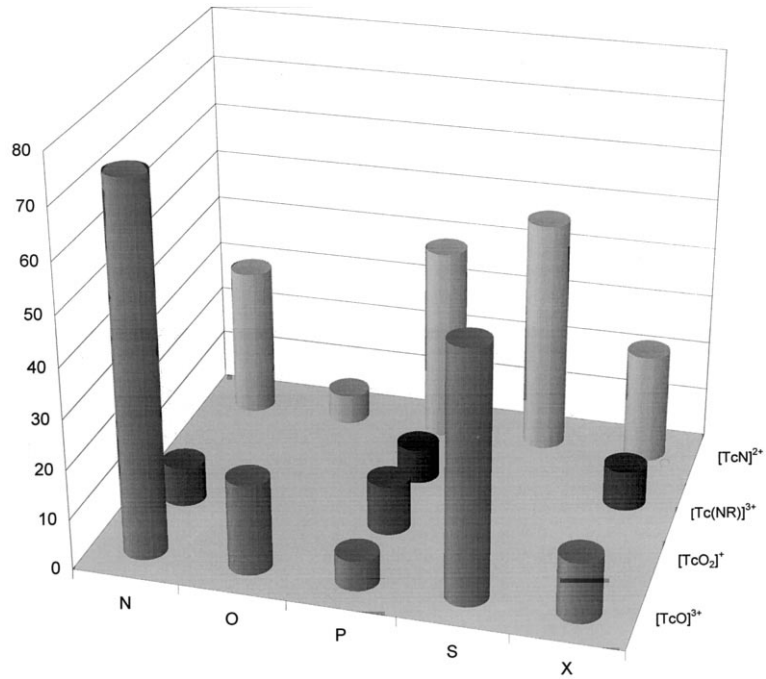

Fig. 33. Distribution of coordinating atoms versus Tc(V) complexes containing distinctive cores. NR denotes the imido group.

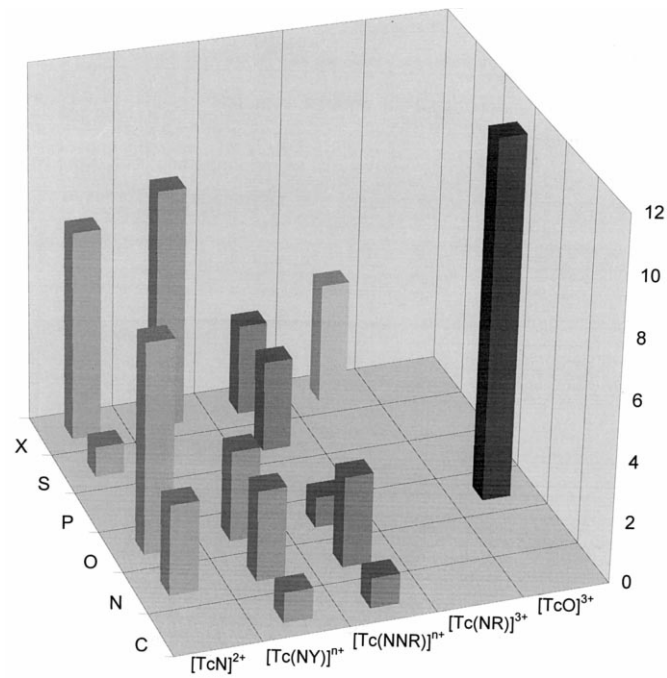

Fig. 34. Occurrence of coordinating atom trans to distinctive core in octahedral Tc complexes. NR, NNR and NY (Y = O, S) denote imido, diazenido and (thio)nitrosyl groups respectively.

On the contrary, mono-oxo complexes select mostly a combination of N and S atoms. More flexible seems to be the nitrido core, which is ligated indifferently by N, S, P and X donors.

The donor atom type located trans to the distinctive core in octahedral complexes is visualized in Fig. 34. In no structure was P found trans to the core, and in only a few cases are C and S exhibited in such a position.

The imido and the mono-oxo groups invariably display a trans-halide and a trans-oxygen coordination respectively. Again, the $[Tc{\equiv}N]^{2+}$ moiety is more versatile in choosing the nature of the trans-donor. As for bond distances around the technetium center, no appreciable variation is detectable compared with the distances already reported in the cumulative table 2 of Ref. [3].

References

[1] F.H. Allen, J.E. Davies, J.J. Galloy, O. Johnson, O. Kennard, C.F. Macrae, E.M. Mitchell, J.M. Smith, D.G. Watson, J. Chem. Info. Comp. Sci. 31 (1991) 187.
[2] G. Bandoli, U. Mazzi, E. Roncari, E. Deutsch, Coord. Chem. Rev. 44 (1982) 57.
[3] F. Tisato, F. Refosco, G. Bandoli, Coord. Chem. Rev. 135–136 (1994) 325.
[4] M. Melnik, J. Van Lier, Coord. Chem. Rev. 77 (1987) 275.
[5] C.E. Housecroft, Coord. Chem. Rev. 146 (1995) 191.
[6] C.E. Housecroft, Coord. Chem. Rev. 162 (1997) 305.
[7] C.E. Housecroft, Coord. Chem. Rev. 169 (1998) 187.
[8] Frost, Sullivan, J. Nucl. Med. 39 (2) (1998) 27N.
[9] Frost, Sullivan, J. Nucl. Med. 39 (3) (1998) 20N.
[10] J.R. Dilworth, S.J. Parrott, Chem. Soc. Rev. 27 (1998) 43.
[11] S. Jurisson, D. Berning, W. Jia, D. Ma, Chem. Rev. 93 (1999) 1137.
[12] S.S. Jurisson, J.D. Lydon, Chem. Rev. 99 (1999) 2205.
[13] S. Liu, D.S. Edwards, Chem. Rev. 99 (1999) 2235.
[14] Y. Arano, Adv. Drug Del. Rev. 37 (1999) 103.
[15] D.L. Nosco, J.A. Beaty-Nosco, Coord. Chem. Rev. 184 (1999) 91.
[16] R. Alberto, R. Schibli, R. Waibel, U. Abram, A.P. Schubiger, Coord. Chem. Rev. 190–192 (1999) 901.
[17] P. Sadler, Z. Guo, Angew. Chem. Int. Ed. Engl. 38 (1999) 1512.
[18] R. Pasqualini, V. Comazzi, E. Bellande, A. Duatti, A. Marchi, Appl. Radiat. Isot. 43 (1992) 1329.
[19] M.J. Abrams, M. Juweid, C.I. Tenkate, D.A. Schwartz, M.M. Hauser, F.E. Gaul, A.J. Fuccello, R.H. Rubin, H.W. Strauss, A.J. Fischmann, J. Nucl. Med. 31 (1990) 2022.
[20] A.W. Addison, T.N. Rao, J. Reedijk, J. Van Rijn, G.C. Verschoor, J. Chem. Soc. Dalton Trans. (1984) 1349.
[21] U. Abram, J.R. Dilworth, Z. Anorg. Allg. Chem. 625 (1999) 609.
[22] J.R. Dilworth, R. Hübener, U. Abram, Z. Anorg. Allg. Chem. 623 (1997) 880.
[23] U. Abram, E. Shulz Lang, S. Abram, J. Wegmann, J.R. Dilworth, R. Kirmse, J.D. Woollins, J. Chem. Soc. Dalton Trans. (1997) 623.
[24] C. Bolzati, E. Malagò, A. Boschi, A. Cagnolini, M. Porchia, G. Bandoli, New J. Chem. 23 (1999) 807.
[25] C. Bolzati, A. Boschi, L. Uccelli, E. Malagò, G. Bandoli, F. Tisato, F. Refosco, R. Pasqualini, A. Duatti, Inorg. Chem. 38 (1999) 4473.
[26] U. Abram, S. Abram, J.R. Dilworth, Z. Anorg. Allg. Chem. 622 (1996) 1257.
[27] F.D. Rochon, R. Melanson, P.-C. Kong, Polyhedron 15 (1996) 2641.
[28] F. Refosco, F. Tisato, A. Moresco, G. Bandoli, J. Chem. Soc. Dalton Trans. (1995) 3475.
[29] A. Marchi, L. Marvelli, M. Cattabriga, R. Rossi, M. Neves, V. Bertolasi, V. Ferretti, J. Chem. Soc. Dalton Trans. (1999) 1937.

[30] G. Cros, H. Belhadj Tahar, D. de Montauzon, A. Gleizes, Y. Coulais, R. Guiraud, E. Bellande, R. Pasqualini, Inorg. Chim. Acta 227 (1994) 25.
[31] Y. Kani, T. Takayama, S. Inomata, T. Sekine, H. Kudo, Chem. Lett. (1995) 1059.
[32] Y. Kani, T. Takayama, T. Sekine, H. Kudo, J. Chem. Soc. Dalton Trans. (1999) 209.
[33] H.-J. Pietzsch, H. Spies, P. Leibnitz, G. Reck, Polyhedron 12 (1993) 2995.
[34] M.B. Gernert, W. Hiller, J.R. Dilworth, S.J. Parrott, Z. Kristallogr. 210 (1995) 961.
[35] U. Abram, R. Alberto, J.R. Dilworth, Y. Zheng, K. Ortner, Polyhedron 18 (1999) 2995.
[36] S. Ritter, U. Abram, J.R. Dilworth, Z. Anorg. Allg. Chem. 622 (1996) 1975.
[37] A. Marchi, R. Rossi, L. Marvelli, V. Bertolasi, Inorg. Chem. 32 (1993) 4673.
[38] A. Marchi, L. Marvelli, R. Rossi, L. Magon, L. Uccelli, V. Bertolasi, V. Ferretti, F. Zanobini, J. Chem. Soc. Dalton Trans. (1993) 1281.
[39] F. Refosco, F. Tisato, G. Bandoli, A. Cagnolini, A. Moresco, C. Bolzati, L. Uccelli, A. Boschi, A. Duatti, in: M. Nicolini, U. Mazzi (Eds.), Technetium, Rhenium and Other Metals in Chemistry and Nuclear Medicine, vol. 5, SGE Editoriali, Italy, 1999, p. 139.
[40] M. Cattabriga, A. Marchi, L. Marvelli, R. Rossi, G. Vertuani, R. Pecoraro, A. Scatturin, V. Bertolasi, V. Ferretti, J. Chem. Soc. Dalton Trans. (1998) 1453.
[41] F. Tisato, F. Refosco, A. Cagnolini, G. Bandoli, C. Bolzati, L. Uccelli, A. Boschi, S. Prakash, A. Duatti, in: M. Nicolini, U. Mazzi (Eds.), Technetium, Rhenium and Other Metals in Chemistry and Nuclear Medicine, vol. 5, SGE Editoriali, Italy, 1999, p. 133.
[42] F. Refosco et al., unpublished results.
[43] B. Lorenz, P. Kränke, K. Schmidt, R. Kirmse, R. Hübener, U. Abram, Z. Anorg. Allg. Chem. 620 (1994) 921.
[44] J. Baldas, S.F. Colmanet, Z. Ivanov, G.A. Williams, J. Chem. Soc. Chem. Commun. (1994) 2153.
[45] M.T. Benson, J.C. Bryan, A.K. Burrell, T.R. Cundari, Inorg. Chem. 34 (1995) 2348.
[46] J.C. Bryan, A.K. Burrell, M.M. Miller, W.H. Smith, C.J. Burns, A.P. Sattelberger, Polyhedron 12 (1993) 1769.
[47] A.K. Burrell, J.C. Bryan, Angew. Chem. Int. Ed. Engl. 32 (1993) 94.
[48] A.K. Burrell, D.L. Clark, P.L. Gordon, A.P. Sattelberger, J.C. Bryan, J. Am. Chem. Soc. 116 (1994) 3813.
[49] A.K. Burrell, J.C. Bryan, Organometallics 12 (1993) 2426.
[50] T. Nicholson, A. Davison, J.A. Zubieta, Q. Chen, A.G. Jones, Inorg. Chim. Acta 230 (1995) 205.
[51] F.D. Rochon, R. Melanson, P.-C. Kong, Inorg. Chem. 34 (1995) 2273.
[52] T. Nicholson, M. Hirsch-Kuchma, A. Davison, A.G. Jones, Inorg. Chim. Acta 271 (1998) 191.
[53] C.M. Archer, J.R. Dilworth, P. Jobanputra, R.M. Thompson, M. McPartlin, W. Hiller, J. Chem. Soc. Dalton Trans. (1993) 897.
[54] J.R. Dilworth, P. Jobanputra, R.M. Thompson, D.C. Povey, C.M. Archer, J.D. Kelly, J. Chem. Soc. Dalton Trans. (1994) 1251.
[55] T. Nicholson, M. Hirsch-Kuchma, A. Davison, W.M. Davies, A.G. Jones, Inorg. Chim. Acta 267 (1998) 165.
[56] D.J. Rose, K.P. Maresca, T. Nicholson, A. Davison, A.G. Jones, J. Babich, A. Fischman, W. Graham, J.R.D. DeBord, J. Zubieta, Inorg. Chem. 37 (1998) 2701.
[57] J. Cook, A. Davison, W.M. Davies, A.G. Jones, Organometallics 14 (1995) 650.
[58] T. Nicholson, M. Hirsch-Kuchma, E. Freiberg, A. Davison, A.G. Jones, Inorg. Chim. Acta 279 (1998) 206.
[59] H.J. Banbery, T.A. Hamor, Acta Crystallogr. Sect. C 50 (1994) 44.
[60] T. Nicholson, M. Hirsch-Kuchma, A. Shellenbarger-Jones, A. Davison, A.G. Jones, Inorg. Chim. Acta 267 (1998) 319.
[61] S. Storm Blanchard, T. Nicholson, A. Davison, W. Davis, A.G. Jones, Inorg. Chim. Acta 244 (1996) 121.
[62] L.C. Francesconi, G. Graczyk, S. Wehrli, S.N. Shaikh, D. McClinton, S. Liu, J. Zubieta, H.F. Kung, Inorg. Chem. 32 (1993) 3114.
[63] A. Mahmood, personal communication.
[64] L.C. Francesconi, Y.Y. Yang, M.-P. Kung, X.X. Zhang, J.J. Billings, Y.-Z. Guo, H.F. Kung, J. Med. Chem. 37 (1994) 3282.

[65] H. Alarabi, R.A. Bell, R. Faggian, H.E. Howard-Lock, C.J.L. Lock, A.V. Kramer, Inorg. Chem. 34 (1995) 1688.
[66] D.J. Canney, J. Billings, L.C. Francesconi, Y.-Z. Guo, B.S. Haggerty, A.L. Rheingold, H.F. Kung, J. Med. Chem. 36 (1993) 1032.
[67] I. Pirmettis, S. Mastrostamatis, M. Papadopoulos, C.P. Raptopoulou, A. Terzis, E. Chiotellis, J. Labelled Compds. Radiopharmaceut. 34 (1994) 817.
[68] B. Johannsen, B. Noll, P. Leibnitz, G. Reck, S. Noll, H. Spies, Inorg. Chim. Acta 210 (1993) 209.
[69] G. Grummon, R. Rajagopalan, G.J. Palenik, A.E. Koziol, D.L. Nosco, Inorg. Chem. 34 (1995) 1764.
[70] N.M. Blaton, G. Bormans, O.M. Peeters, A. Verbruggen, Acta Crystallogr. Sect. C 53 (1997) 449.
[71] G. Bormans, O.M. Peeters, H. Vanbilloen, N. Blaton, A. Verbruggen, Inorg. Chem. 35 (1996) 6240.
[72] C.-S. Tsai, T.-H. Lu, J.-Y. Duh, S.-J. Yeh, Acta Crystallogr. Sect. C 52 (1996) 838.
[73] K.E. Linder, Y.-W. Chan, J.E. Cyr, M.F. Malley, D.P. Nowotnik, A.D. Nunn, J. Med. Chem. 37 (1994) 9.
[74] F. Tisato, F. Refosco, A. Moresco, G. Bandoli, A. Dolmella, C. Bolzati, Inorg. Chem. 34 (1995) 1779.
[75] S.G. Mastrostamatis, M.S. Papadopoulos, I.C. Pirmettis, E. Paschali, A.D. Varvarigou, C.I. Stassinopoulou, C.P. Raptopoulou, A. Terzis, E. Chiotellis, J. Med. Chem. 37 (1994) 3212.
[76] I.C. Pirmettis, M.S. Papadopoulos, S.G. Mastrostamatis, C.P. Raptopoulou, A. Terzis, E. Chiotellis, Inorg. Chem. 35 (1996) 1685.
[77] D.M. Spyriounis, M. Pelecanou, C.I. Stassinopoulou, C.P. Raptopoulou, A. Terzis, E. Chiotellis, Inorg. Chem. 34 (1995) 1077.
[78] M.S. Papadopoulos, M. Pelecanou, I.C. Pirmettis, D.M. Spyriounis, C.P. Raptopoulou, A. Terzis, C.I. Stassinopoulou, E. Chiotellis, Inorg. Chem. 35 (1996) 4478.
[79] H. Luo, S.J. Rettia, C. Orvig, Inorg. Chem. 32 (1993) 4491.
[80] H.-J. Pietzsch, H. Spies, P. Leibnitz, G. Reck, J. Beger, R. Jacobi, Polyhedron 12 (1993) 187.
[81] F.D. Rochon, R. Melanson, P.-C. Kong, Inorg. Chim. Acta 254 (1997) 303.
[82] E. Shuter, H.R. Hoveyda, V. Karunaratne, S.J. Rettig, C. Orvig, Inorg. Chem. 35 (1996) 368.
[83] C. Bolzati, F. Tisato, F. Refosco, G. Bandoli, Inorg. Chim. Acta 247 (1996) 125.
[84] F. Refosco, F. Tisato, G. Bandoli, C. Bolzati, A. Dolmella, A. Moresco, M. Nicolini, J. Chem. Soc. Dalton Trans. (1993) 605.
[85] T. Gerber, H. Kemp, J. Du Preez, G. Bandoli, Radiochim. Acta 63 (1993) 129.
[86] C. Kremer, J. Gancheff, E. Kremer, A.W. Mombrù, O. Gonzalez, R. Mariezcurrena, L. Suescun, M.L. Cubas, O.N. Ventura, Polyhedron 16 (1997) 3311.
[87] F.D. Rochon, R. Melanson, P.-C. Kong, Inorg. Chem. 37 (1998) 87.
[88] U. Abram, S. Abram, H.R. Macke, P. Koch, Z. Anorg. Allg. Chem. 61 (1995) 854.
[89] J. Lu, C.D. Hiller, M.J. Clarke, Inorg. Chem. 32 (1993) 1417.
[90] J. Barrera, J.C. Bryan, Inorg. Chem. 35 (1996) 1825.
[91] F. Tisato, F. Refosco, G. Bandoli, C. Bolzati, A. Moresco, J. Chem. Soc. Dalton Trans. (1994) 1453.
[92] H. Spies, M. Glaser, H.-J. Pietzsch, F.E. Hahn, O. Kintzel, T. Lügger, Angew. Chem. Int. Ed. Engl. 33 (1994) 1354.
[93] F. Mevellec et al., unpublished results.
[94] B. Lorenz, K. Schmidt, W. Hiller, U. Abram, R. Hübener, Inorg. Chim. Acta 208 (1993) 195.
[95] F. Tisato, C. Bolzati, A. Duatti, G. Bandoli, F. Refosco, Inorg.Chem. 32 (1993) 2042.
[96] R.A. Bell, J.F. Britten, A. Guest, C.J.L. Lock, J.F. Valliant, J. Chem. Soc. Chem. Commun. (1997) 585.
[97] F.D. Rochon, R. Melanson, P.-C. Kong, Inorg. Chim. Acta 245 (1996) 251.
[98] L. Kaden, A.J.L. Pombeiro, Y. Wang, U. Abram, Inorg. Chim. Acta 230 (1995) 189.
[99] A.K. Burrell, J.C. Bryan, G.J. Kubas, Organometallics 13 (1994) 1067.
[100] F.A. Cotton, S.C. Haefner, A.P. Sattelberger, J. Am. Chem. Soc. 118 (1996) 5486.
[101] C.M. Archer, J.R. Dilworth, R.M. Thompson, M. McPartlin, D.C. Povey, J.D. Kelly, J. Chem. Soc. Dalton Trans. (1993) 461.

[102] J. Barrera, A.K. Burrell, J.C. Bryan, Inorg. Chem. 35 (1996) 335.
[103] J.C. Bryan, F.A. Cotton, L.M. Daniels, S.C. Haefner, A.P. Sattelberger, Inorg. Chem. 34 (1995) 1875.
[104] T. Malyusz, W. Preetz, Z. Anorg. Allg. Chem. 622 (1996) 1006.
[105] U. Abram, S. Abram, J.R. Dilworth, Acta Crystallogr. Sect. C 52 (1996) 605.
[106] F. Refosco, F. Tisato, G. Bandoli, E. Deutsch, J. Chem. Soc. Dalton Trans. (1993) 2901.
[107] R. Hübener, U. Abram, W. Hiller, Acta Crystallogr. Sect. C 50 (1994) 188.
[108] K.-I. Okamoto, B. Chen, J.R. Kirchhoff, D.M. Ho, R.C. Elder, W.R. Heineman, E. Deutsch, M.J. Heeg, Polyhedron 12 (1993) 1559.
[109] T. Konno, R. Seeber, J.R. Kirchhoff, W.R. Heineman, E. Deutsch, M.J. Heeg, Transition Met. Chem. 18 (1993) 209.
[110] K.-I. Okamoto, J.R. Kirchhoff, W.R. Heineman, E. Deutsch, M.J. Heeg, Polyhedron 12 (1993) 749.
[111] F.D. Rochon, R. Melanson, P.-C. Kong, Can. J. Chem. 72 (1994) 2183.
[112] U. Abram, S. Abram, J.R. Dilworth, Acta Crystallogr. Sect. C 51 (1995) 1983.
[113] F.D. Rochon, R. Melanson, Acta Crystallogr. Sect. C 49 (1993) 1259.
[114] S. Jurisson, M.M. Halihan, J.D. Lydon, C.L. Barnes, D.P. Nowotnik, A.D. Nunn, Inorg. Chem. 37 (1998) 1922.
[115] H. Li, X. Wang, Q. Yang, W. Zhou, Y. Wu, Y. Liu, Radiochim. Acta 63 (1993) 213.
[116] E.H. Treher, L.F. Francesconi, M.F. Malley, J.Z. Gougoutas, A.D. Nunn, Inorg. Chem. 28 (1989) 341.
[117] A.K. Burrell, J.C. Bryan, G.J. Kubas, J. Am. Chem. Soc. 116 (1994) 1575.
[118] R. Alberto, R. Schibli, P.A. Schubiger, U. Abram, T.A. Kaden, Polyhedron 15 (1996) 1079.
[119] R. Alberto, R. Schibli, A. Egli, P.A. Schubiger, W.A. Herrmann, G. Artus, U. Abram, T.A. Kaden, J. Organomet. Chem. 493 (1995) 119.
[120] M.S. Grigoriev, S.V. Kryutchkov, Radiochim. Acta 63 (1993) 187.
[121] R. Alberto, R. Schibli, A.P. Schubiger, U. Abram, H.-J. Pietzsch, B. Johannsen, J. Am. Chem. Soc. 121 (1999) 6076.
[122] U. Abram, S. Abram, R. Schibli, R. Alberto, J.R. Dilworth, Polyhedron 17 (1998) 1303.
[123] J.E. Joachim, C. Apostolidis, B. Kanellakolulos, R. Maier, N. Marques, D. Meyer, J. Müller, A. Pires de Matos, B. Nuber, J. Rebizant, M.L. Ziegler, J. Organomet. Chem. 448 (1993) 119.
[124] R. Schibli, R. Alberto, U. Abram, S. Abram, A. Egli, P.A. Schubiger, T.A. Kaden, Inorg. Chem. 37 (1998) 3509.
[125] R. Alberto, R. Schibli, D. Angst, P.A. Schubiger, U. Abram, S. Abram, T.A. Kaden, Transition Met. Chem. 22 (1997) 597.
[126] R. Alberto, R. Schibli, P.A. Schubiger, U. Abram, R. Hübener, H. Berke, T.A. Kaden, J. Chem. Soc. Chem. Commun. (1996) 1291.
[127] J.E. Joachim, C. Apostolidis, B. Kanellakopulos, D. Mayer, K. Raptis, J. Rebizant, M.L. Ziegler, J. Organomet. Chem. 476 (1994) 77.
[128] J.E. Joachim, C. Apostolidis, B. Kanellakopulos, R. Maier, D. Meyer, J. Rebizant, M.L. Ziegler, J. Organomet. Chem. 455 (1993) 137.
[129] J.E. Joachim, C. Apostolidis, B. Kanellakopulos, D. Meyer, B. Nuber, K. Raptis, J. Rebizant, M.L. Ziegler, J. Organomet. Chem. 492 (1995) 199.
[130] E.O. Fischer, C. Apostolidis, E. Dornberger, A.C. Filippou, B. Kanellakopulos, B. Lungwitz, J. Muller, B. Powietzka, J. Rebizant, W. Roth, Z. Naturforsch. Teil B 50 (1995) 1382.
[131] E. Freiberg, A. Davison, A.G. Jones, W.M. Davies, Inorg. Chem. Commun. 2 (1999) 516.
[132] F.A. Cotton, L.M. Daniels, S.C. Haefner, A.P. Sattelberger, Inorg. Chim. Acta 288 (1999) 69.
[133] C.J. Burns, A.K. Burrell, F.A. Cotton, S.C. Haefner, A.P. Sattelberger, Inorg. Chem. 33 (1994) 2257.
[134] F.A. Cotton, S.C. Haefner, A.P. Sattelberger, Inorg. Chem. 35 (1996) 1831.
[135] F.A. Cotton, S.C. Haefner, A.P. Sattelberger, Inorg. Chem. 35 (1996) 7350.
[136] F.A. Cotton, S.C. Haefner, A.P. Sattelberger, Inorg. Chim. Acta 266 (1997) 55.
[137] N.A. Baturin, M.S. Grigoriev, S.V. Kryutchkov, V.G. Maksimov, Koord. Khim. 20 (1991) 671.
[138] B. Eble, D. Berning, C.L. Barnes, K.V. Katti, S. Jurisson, J. Chem. Crystallogr. 29 (1999) 39.

[139] M.S. Grigoriev, S.V. Kryutchkov, V.G. Maksimov, Yu.T. Struchkov, A.I. Yanovsky, Koord. Khim. 20 (1994) 870.
[140] B.G. Antipov, S.V. Kryuchkov, V.N. Gerasimov, M.S. Grigoriev, P.E. Kazin, V.V. Karitonov, V.G. Maksimov, S.V. Moisa, V.V. Sergeev, T.K. Yurik, Koord. Khim. 21 (1995) 716.
[141] B.N. Figgis, P.A. Reynolds, F.K. Larsen, G.A. Williams, C.D. Delfs, Aust. J. Chem. 49 (1996) 633.
[142] J. Baldas, J.F. Boas, S.F. Colmanet, A.D. Rae, G.A. Williams, Proc. R. Soc. London Ser. A 442 (1993) 437.
[143] U. Abram, R. Hubener, R. Wollert, R. Kirmse, W. Hiller, Inorg. Chim. Acta 206 (1993) 9.
[144] H.P.A. Mercier, G.J. Schrobilgen, Inorg. Chem. 32 (1993) 145.
[145] W.J. Casteel, Jr., D.A. Dixon, N. LeBlond, H.P.A. Mercier, G.J. Schrobilgen, Inorg. Chem. 37 (1998) 340.
[146] W. Bronger, M. Kanerty, M. Loeverich, D. Schmitz, K. Schwochau, Angew. Chem. Int. Ed. Engl. 32 (1993) 576.
[147] H.-J. Lamfers, A. Meetsma, G.A. Wiegers, J.L. de Boer, J. Alloys Compds. 241 (1996) 34.
[148] M.S. Grigorev, A.E. Miroslavov, G.V. Sidorenko, D.N. Suglobov, Radiochemistry 39 (1997) 202.
[149] B. Noll, P. Leibnitz, H. Spies, Forschungszentrum Rossendorf (FZR), Report 270, 1998/99, p. 151.
[150] G. Patsis, I.C. Pirmettis, M.S. Papadopoulos, C.P. Raptopoulou, A. Terzis, E. Chiotellis, J. Labelled Compds. Radiopharmaceut. 42 (1999) 255.
[151] B. Noll, P. Leibnitz, H. Spies, Forschungszentrum Rossendorf (FZR), Report 270, 1998/99, p. 153.
[152] H.J. Pietzsch, S. Seifert, A. Drews, P. Leibnitz, H. Spies, Forschungszentrum Rossendorf (FZR), Report 283, 1999, p. 74.
[153] H.J. Pietzsch, A. Gupta, R. Syhre, H. Spies, Forschungszentrum Rossendorf (FZR), Report 283, 1999, p. 84.
[154] U. Abram, Z. Anorg. Allg. Chem. 626 (2000) 1.